GCAGS JOURNAL
A Publication of the Gulf Coast Association of Geological Societies
www.gcags.org

INVESTIGATION OF THE *CORBULA* BED OF CENTRAL TEXAS AS THE PRODUCT OF CATASTROPHIC TSUNAMI DEPOSITION

Roger Sigler[1], Heather Fell[2], Brenda L. Kirkland[3], and C. Van Wingerden[4]

[1]*19114 Treetoad Dr., Katy, Texas 77449, U.S.A.*

[2]*8150 County Rd. 436, #100, Princeton, Texas 75407, U.S.A.*

[3]*Department of Geosciences, Mississippi State University, P.O. Box 5448, Starkville, Mississippi 39762, U.S.A.*

[4]*P.O. Box 902, Lake Isabella, California 93240, U.S.A.*

ABSTRACT

Corbulids are tiny clams that live in low energy environments. They are elongate, up to about 7 mm in length, prefer fine grained sediments, and they burrow nearly vertical with their pointy posterior up. In Central Texas, the *Corbula* bed covers an area of 13,000 km^2 and is generally no more than 1 m thick. The geologic setting of a very wide backreef lagoon was the ideal setting for corbulids to prosper as their vast numbers and sizes testify. Their articulated nature within supercritical flow bedforms indicates that they were transported and deposited alive by high velocity currents. The *Corbula* bed can be divided into two layers. The lower half consists of a hard, dense iron-stained medium to very coarse packstone beds with load features and supercritical flow structures including antidunes, wavy plane beds, and a traction carpet above an erosive sharp undulating contact at the base. The upper half is a soft, friable crudely laminated to massive wackestone-packstone with increasing mud content. Storms and storm-generated tides were discounted because they rarely produce and preserve antidunes, and they are limited to much smaller geographical areas of intertidal beaches and storm washover fans. Outcrops confirm at least 4000 km^2 of antidunes in the lower half of the *Corbula* bed. Antidunes rarely preserve in nature unless there are diversions of the current and rapid burial by continuous sedimentation. The stacking pattern of antidunes in the lower part followed by crudely laminated muddy deposits in the upper part is characteristic of tsunamis. In the lower half, there are two or more antidune beds in quick succession with diverging currents. The flow in lower antidunes was initially towards the west, then south and is interpreted as tsunami drawdown. Antidune remnants at Canyon Lake Gorge indicate that the overriding northeastward flowing tsunami current was rotated towards the north by another strong current from the south. Based on outcrop evidence of the *Corbula* bed, the tsunami flood was at least 40 km wide and flowed at least 90 km in the northeasterly direction. The velocity of the tsunami above the sea floor is estimated between 5–8 m/s with sloshing and seiche as the tsunami waned. The debris that formed the overlying soft wackestone-packstone rapidly fell out of suspension to preserve the antidunes. There is a high probability that submarine earthquakes triggered the tsunami. Several major tectonic structures were located southwest of the study area. In Kendall County, a debris flow with load features and sand volcanoes formed by liquefaction on a low-angle slope of <0.05°. The overriding antidune bed, with wavelengths approaching 60 cm, superimposed above the debris flow bed indicate that high velocity currents were initiated in conjunction with the debris flow.

INTRODUCTION

The Lower Cretaceous Glen Rose Formation is part of the Trinity Group (Stricklin et al., 1971; Ward and Ward, 2007). It is subdivided into the Upper Glen Rose and Lower Glen Rose by the *Corbula* bed, a thin, extensive sheet-like deposit, which blankets an area of at least 13,000 km^2 (Stricklin et al., 1971; Perkins, 1974). The innumerable corbulids, a clam of the Corbulidae family, in the bed are tiny elongate bivalves, with the right valve slightly larger than the left and resemble wheat grains (Whitney, 1952). By convention, the numerous alternating bed types within the Glen Rose Formation have been classically interpreted as transgressive and regressive cycles and sequences (Lozo and Stricklin, 1956; Nagle, 1968; Stricklin et al., 1971; Ward and Ward, 2007). Some researchers assume a quiescent depositional environment overall for the Glen Rose Formation due to the carbonate nature of the formation (Lozo and Stricklin, 1956; Stricklin et al., 1971). However, within the Glen Rose cycles are bedforms indicative of a much more energetic environment. In the

Manuscript received March 31, 2020; revised manuscript received May 4, 2020; manuscript accepted June 17, 2020.

GCAGS Journal, v. 10 (2021), p. 1–23.

Corbula bed, high energy bedforms including asymmetrical current ripples, lenticular bedforms, and articulated bivalves have been noted by others (e.g., Scott, 2007; Scott et al., 2007; Stricklin et al., 1971). The bivalve alignment and articulated nature (both valves being locked together) coupled with their abundance in lenticular beds led Scott (2007) to conclude that the corbulids were rapidly transported alive in a stressful environment. When one thinks of high energy in a lagoon, major storms are usually cited as they are known to rapidly transport significant amounts of sediments (Bebout and Loucks, 1983). High density currents are needed to transport live bivalves, which are covered immediately so that they remain articulated (Försich and Pan, 2016). Tsunamis transport and redeposit sediments over large regions, and their preservation potential is high in lagoons because they are normally calm environments (Sugawara et al., 2008; Peters and Jaffe, 2010). Large tsunamis must leave a geologic record (Bourgeois, 2009).

Marker beds are often the result of catastrophic processes and form the basis of the neo-catastrophist view of the geologic record, which bears evidence of "long periods of boredom and short periods of terror" (Ager, 1993). A tsunami event bed can be an excellent key bed and time marker horizon (Shiki et al, 2008b). The goal of this study is to present a sedimentological case that the *Corbula* bed was likely deposited by tsunami currents. One of the primary diagnostic features of a tsunami deposit is the sheet sand (e.g., Fujiwara, 2008; Goto et al., 2008; Peters and Jaffe, 2010). The *Corbula* bed is exceptionally thin for its wide extent and thereby has the sheet-like geometry of a potential tsunami deposit. Sheets deposited by tsunamis are variable over large distances and can include pebbles to boulders, stacks of beds, shell/bivalve beds, turbid flow structures, and distal units that may just include mud (Fujino, et al., 2008; Fujiwara, 2008; Fujiwara and Kamataki, 2008; Goto et al., 2008; Sugawara et al., 2008). Specific sedimentary structures include graded beds, reverse graded beds, scour-and-fill structures, dunes, antidunes, ripple forms, plane beds, wavy beds, laminations, massive units, and HCS (hummocky cross-stratification) mimics (e.g., Fujiwara, 2008; Shiki et al., 2008b; Bourgeois, 2009; Peters and Jaffe, 2010; Phantuwongraj and Choowong, 2012). Earlier hypotheses about the *Corbula* bed occurred prior to detailed studies of the geologic effects caused by tsunamis. Most studies began in the late 1990s. Since that time, knowledge has greatly increased to the point that a geological textbook on tsunamis was published recently (Shiki et al., 2008) and the analysis of several tsunamis including the 2004 Indian Ocean tsunami was compiled by the U.S. Geological Survey (Peters and Jaffe, 2010). Thus, the geologic effects and depositional bedforms caused by tsunamis is a very recent subset of geology. Specific objectives include (1) a review of geologic work and consequences of tsunamis; (2) analysis of observed sedimentary structures; and (3) proposed causes to trigger tsunamis along this ancient coast.

METHODS

To justify a tsunami interpretation, an analysis of particles and sedimentary structures blanketing such a large region was pursued. To accomplish the task, outcrops were examined, measured, and photographed across several counties where the *Corbula* bed can be seen in several cliffs of river valleys and roadcuts west of Austin and north and northwest of San Antonio (Fig. 1; Table 1). The primary researcher identified sites by use of the larger scale map drawings provided by Perkins (1974). In addition, the geologic maps of Barnes (1967, 1974, 1981, 1982) were helpful with some sites. Stratigraphy of the *Corbula* bed was evaluated along with the contacts of underlying and overlying strata where visible. Attention was given to bedforms, sedimentary structures, and paleocurrent direction(s) with a Brunton compass.

Samples from each of the study locations were cut, polished, and examined for texture, grain types, grain sizes, and patterns utilizing enhanced macrophotography. Macrophotographs of cross-section cuts are upright with the top up. Color inversion enhanced key features of select samples. Standard petrographic analysis of thin sections from other samples aided the interpretation along with photomicrographs. Identification of key foraminifera are noted as being an effective method for the geologic setting and interpreting the sources of tsunami sediments (Putra et al., 2013).

For sedimentary flow processes, Folk (1980) recognized that some researchers considered clastics or detrital debris to include terrigenous and allochemical sources. Depending on location, the *Corbula* bed is described as grainstones, packstones, wackestones, and mudstones (Perkins, 1974; Ward and Ward, 2007). Because a tsunami deposit is described as a sheet sand, most particles should be in the sand sizes range between 0.063 mm to 2 mm for carbonates. An enhanced system was devised with the 2 mm upper boundary for sand-size carbonate particles (e.g., Asquith, 1979; Selley, 1982; Lewis and McConchie, 1994). In this system, more than 90% of particles in grainstones and packstones are less than 2 mm; they were carbonate sands when deposited. Although not as rounded as terrigenous sand, many corbulids are much larger than 2 mm and larger particles do require higher erosion velocities. Whitney (1952) related the average maximum dimensions of corbulids to be: height = 3 mm, length = 7 mm, and width = 1 mm. An average of the three dimensions equates to more than 3 mm, which falls in the 2-4 mm size range of granules (Folk, 1980). Velocity evaluations will be based on the Hjulström diagram in Thornton (1978). A wackestone is essentially a dirty, or muddy, limestone with silt or sand size particles, often with allochems or bioclasts suspended in the finer matrix.

GEOLOGIC SETTING

Deposition of the Glen Rose Formation occurred along the second circum-Gulf carbonate shelf that extended from Florida to Mexico (Scott et al., 2007). During the early Albian stage of the Cretaceous System, the Llano Uplift was a low island or islands on the Central Texas Platform (Plummer, 1950; Bebout and Loucks, 1974; Scott et al., 2007). Based on core analysis of several wells and seismic sections of the Stuart City Trend, Bebout and Loucks (1974) produced a facies model of the depositional environments around the island(s) to the shelf edge. The Stuart City Trend is the narrow band of reefs, banks, bars, and islands that comprised the shelf edge. This trend strikes southwest to northeast and is located about 160 km south-southeast of the Llano island(s). A back-reef shelf lagoon developed between the Llano island and the shelf edge (Stricklin et al., 1971; Bebout and Loucks, 1974; Perkins, 1974; Asquith, 1979). Deposition of the *Corbula* bed occurred within this semi-confined lagoon during the early Albian (Fig. 2). It is possible that when the *Corbula* bed was deposited that the water depth in the lagoon was still 6 m or less (e.g., Bebout and Loucks, 1974). The Hensel Sand, a facies equivalent of the Lower and Upper Glen Rose was deposited alongside the Llano island(s) (Stricklin et al., 1971; Barnes, 1981).

In a broad sense the *Corbula* bed marks a change between the Upper and Lower Glen Rose. In the subsurface, it occurs beneath evaporite beds (Lozo and Stricklin, 1956; Stricklin et al., 1971; Pitman, 1989). The anhydrite and gypsum beds are traceable in the subsurface all around the Llano Uplift and occur as solution beds in outcrop (Stricklin et al., 1971; Pitman, 1989). Because corbulids occur beneath evaporites and within local stringers between gypsum beds led to the belief that the "clams had a high tolerance for hypersaline waters" (Stricklin et al., 1971, their page 28). About 100 km northeast of the Llano island(s), the middle unit of the "*Corbula*-bed cycle" in the Paluxy River valley has been equated with the *Corbula* bed of Central

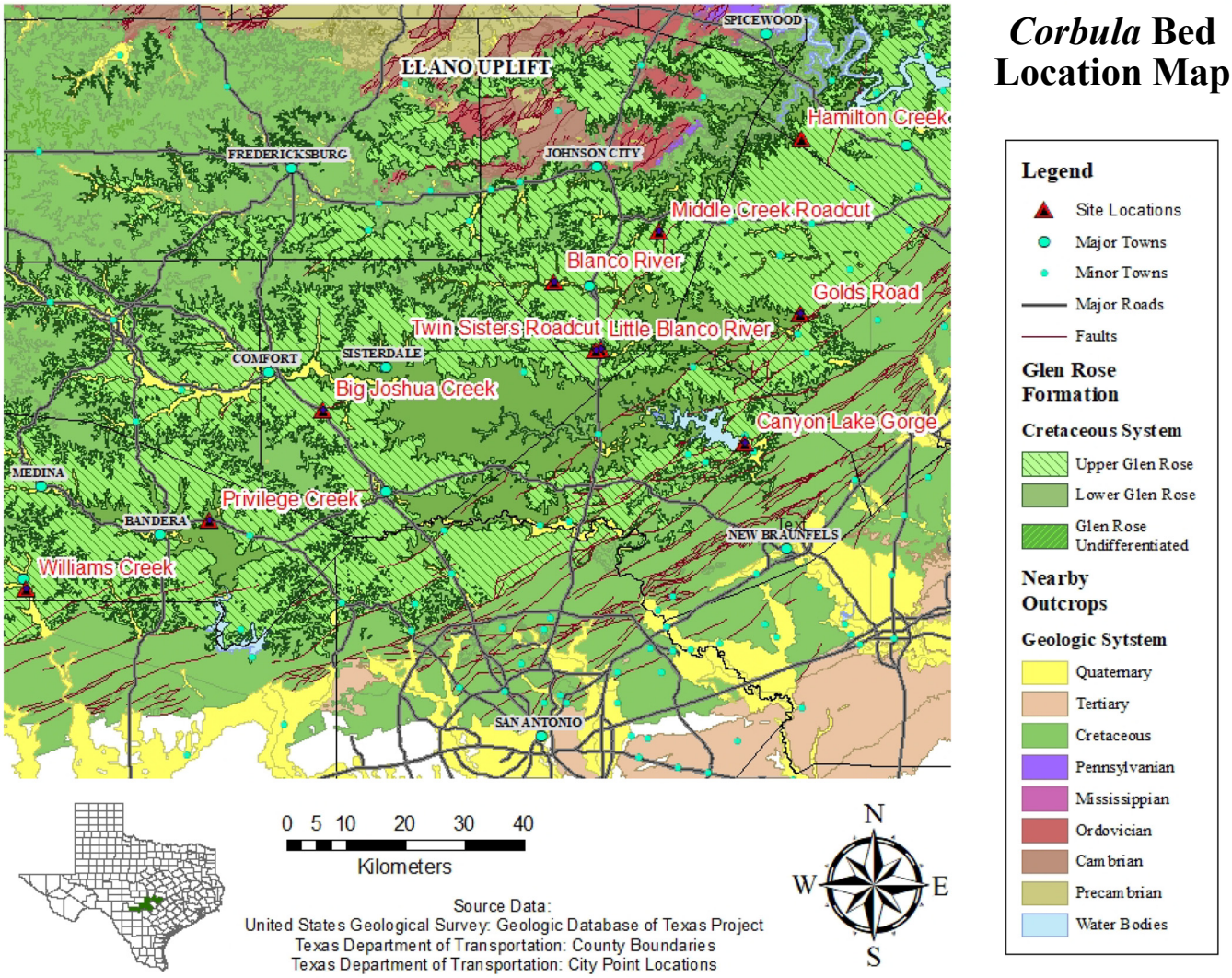

Figure 1. Geologic map with study locations. Datum is the World Geodetic System of 1984 (WGS84).

Table 1. Global positioning system coordinates of site locations. Projected coordinate datum is World Geodetic System 84 (WGS 84). The handheld GPS unit utilized is the Commander Compass App (http://happymagenta.com/compass/) on an Apple iPhone 7.

Location Name	County	Latitude	Longitude
Big Joshua Creek	Kendall	29.91055556	-98.82416667
Blanco River	Blanco	30.10444444	-98.47555556
Canyon Lake Gorge	Comal	29.86138889	-98.18916667
Golds Road (Woodcreek, Texas)	Hays	30.05694	-98.1044
Hamilton Creek	Travis	30.31916667	-98.10333333
Little Blanco River	Blanco	30.00178333	-98.41305556
Middle Creek Roadcut	Blanco	30.17944444	-98.31722222
Privilege Creek	Bandera	29.7458333	-98.99527778
Twin Sisters Roadcut	Blanco	30.00361111	-98.40527778
Williams Creek (Wilson Property)	Bandera	29.6425	-99.27111111

Texas (Nagle, 1968, his page 9). The +/- 20 cm thick bed is the only one with articulated corbulids that align perpendicular to ripple strike with good sorting in a shell hash. Nagle (1968) felt that the ripples must have formed by waves in an intertidal environment near and at the beach. This along with the presence of thick-shelled ostracods in the deposit and tiny gypsum crystals in the overlying unit led to an interpretation of hypersaline waters in that area.

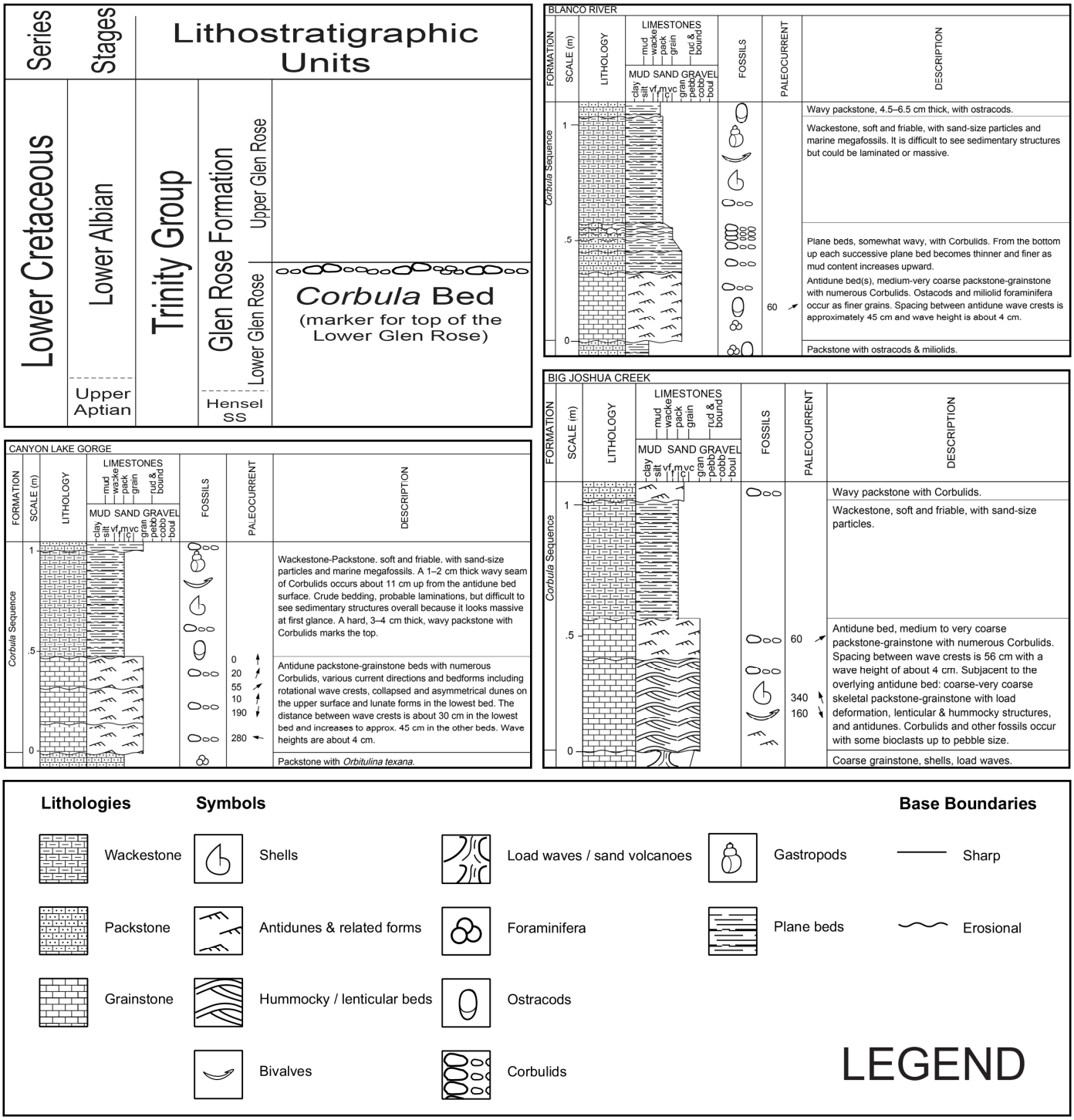

Figure 2. Stratigraphic setting and measured sections of the *Corbula* bed. Because it is a multibed form at these locations, it is called the *Corbula* sequence, which is +/- 1 m thick overall at each of these locations.

In Central Texas, the *Salenia* interval, a transgressive deposit, occurs beneath the *Corbula* bed (Ward and Ward, 2007). South of the Llano island within 80 km of the Llano shoreline (the same region as the present study) salinity was lower than normal in the *Salenia* beds (Perkins, 1974). Runoff carried terrigenous sediments from the Llano Uplift and into the sea where they were transported southwestward by gentle marine currents (Perkins, 1974). Orientation of ripples, coral distribution, and the northeast to southwest decrease in grain size of the terrigenous clastics in the *Salenia* beds exhibit evidence for a current that flowed from the northeast to the southwest (Perkins, 1974). Salinity to the northeast was closer to normal marine than to the southwest because it contained more coral (Perkins, 1974). Thus, Perkin (1974) envisioned that normal marine waters originated from the East Texas Embayment and flowed southwestward across an initially brackish lagoon. Salinity increased while the transgressive *Salenia* beds were being deposited.

In all places, Perkins (1974) placed the *Corbula* bed directly above the *Salenia* interval, which seems to coincide with the extent of the *Corbula* bed. Corbulids may have originated in the

southwest because the fossil has been discovered in the *Salenia* beds of Bandera and Kendall counties (Perkins, 1974). Although difficult to find, corbulids have been observed in the *Salenia* beds by the primary researcher at Privilege Creek, Bandera County. Small clam borings in intertidal rocks (evidenced by mudcracks and dinosaur tracks) beneath the *Salenia* beds of Bandera and Uvalde counties may have been made by corbulids (Stricklin et al., 1971). Perkins (1974) also claimed that there is a consistent relationship with an overlying solution collapse breccia. He showed this on his Hondo Creek section in Bandera County where solution collapse occurred about 1 m above the top of the *Corbula* bed. Hypersaline conditions arose in the upper Glen Rose (Barker et al., 1994). The *Corbula* bed may be the key to the change.

STRATIGRAPHY AND SEDIMENTARY STRUCTURES

Most modern tsunami deposits display a sharp, irregular, undulating erosional basal contact (Fujiwara, 2008; Sugawara et al., 2008; Peters and Jaffe, 2010). The contact is considered disconformable (Keating et al., 2008). In a subaqueous environment, a multiple bed type sand sheet is typical (Fujiwara, 2008). Modern tsunami sheet sands usually have up to 4 beds stacked above the sharp contact; 2 layers are common but up to 7 layers have been documented (Peters and Jaffe, 2010). Individual beds range from 1 cm to 30 cm with a maximum overall thickness of 1.5 m. In the tropics, the chief constituent is carbonate sand (Peters and Jaffe, 2010). Preservation and deposition of all beds within a sand sheet may not exist at all locations because of differences in flow velocities, viscosity, local geology, and geomorphology of the seabed (Fujiwara, 2008).

The type locality of the *Corbula* bed in Central Texas is located about 10 km north of Wimberly, Texas, along Highway 12 (Whitney, 1952; Scott, 2007). At this location, the *Corbula* bed is 30–38 cm thick packed full of corbulids (Whitley, 1952). The Highway 12 location is inaccessible; however, with some effort the *Corbula* bed can be seen nearby in a few weathered roadcuts along Golds Road, which proceeds westward from Highway 12 on the northside of Woodcreek, Texas (Fig. 1; Table 1). At Golds Road, the *Corbula* bed is hard, iron-stained and about 15 cm thick. A mound-shape or hummock sample with abundant corbulids was found in the float. Whitney's (1952) description matches the bed elsewhere. This is primarily true of the ubiquitous hard, iron-stained ledge-forming bed that has been accurately traced across the study in aerial photographs (Stricklin et al., 1971; Perkins, 1974). Apparently, this hard, iron-stained traceable bed corresponds to the type locality, which is equivalent to the lower half of the *Corbula* sequence (Fig. 2). It is called a sequence in Figure 2 because the *Corbula* "bed" is a multibed form. Perkins (1974) denoted it as *Corbula* beds in plural on his measured sections of the Lower Glen Rose. Others called it the *Corbula* interval (Ward and Ward, 2007). The term "interval" is avoided because of its genetic implications regarding time, because if rapid processes did produce the *Corbula* multibed form, then nongenetic terminology is preferred. In total, then, the *Corbula* sequence measures +/- 1 m as indicated in Figure 2, which are the findings of previous researchers (e.g., Perkins, 1974; Ward and Ward, 2007). The upper half of the *Corbula* sequence, to be discussed later, is a soft, friable wackestone-packstone and does not occur everywhere.

The thickness of the iron-stained *Corbula* bed or type bed varies with location and even over short distances at the same location. The primary reason for this is the undulating sharp erosion surface, often concave-up, at the contact with the underlying beds. This situation is observable at most locations such as the Middle Creek roadcut (Fig. 3). The Middle Creek roadcut occurs along Middle Creek Road about 2–3 km south of Highway 290, several kilometers east of Johnson City, Texas. Middle Creek is a tributary to Miller Creek, the latter of which parallels Highway 290. It is the same location as section VI of the compiled Miller Creek section of Perkins (1974) and can be confirmed on the Yeager Quadrangle (Barnes, 1967). After crossing the low water bridge, the site occurs east of the creek up the steep hill and around a sharp bend. The roadcut occurs on both sides of the road and is in excellent condition for study. As indicated in Figure 3, the thickness of the iron-stained *Corbula* type bed changes from 10-40 cm over short distances. It was deposited above *Orbitulina texana* bearing packstone beds, which appears not to have been lithified at the time. It has a sharp, erosional undulating surface at the contact. Rip up clasts, sole marks, load structures, and deep penetrating gouges occur (Fig. 4). Differential loading with sole marks at the contact is an indicator of turbulent flow (Dott and Bourgeois, 1982). Whitish elongate elliptical fossil bioclasts can be readily observable on the surface of the bed. At first glance they look like corbulids, but instead they are *Orbitulina texana* bioclasts, which were likely derived from the underlying beds. Corbulids seem to be rare at this location. The deep gouge of Figure 4 could represent loading combined with scour-and-fill processes that placed the *Orbitulina* bioclasts into the *Corbula* bed. Tsunamis are known to leave "pronounced scour pits" (Keating et al., 2008, p. 370). *Orbitulina texana* bearing beds have also been observed beneath the *Corbula* bed at the Golds Road and Canyon Lake Gorge locations. Small linguoid bed waves on the surface strike at 150–180° with the steep side facing east-northeast indicating a paleoflow in that direction. These could be the small bed waves that occur on the surface of three-dimensional antidunes (Alexander et al., 2001).

The type bed just described corresponds to the lower half of the *Corbula* sequence at Big Joshua Creek, Canyon Lake Gorge, and the Blanco River sites (Fig. 2). As Figure 2 shows, the lower half of the *Corbula* sequence at Big Joshua Creek is 0.5 m thick and is subdivided into a thicker basal bed averaging to no more than 35 cm in thickness and the ubiquitous overlying iron-stained bed +/- 15 cm thick. The basal bed features an abundance of corbulid steinkerns, load deformation features, lenticular structures and mound-shape bed wave forms interpreted as antidunes (Fig. 5). The dark gray load casts or load-flow structures (Fig. 5A) are jointed and have a repetitive concave up surface, which is more evident in the foreground of the photograph (the layer in the background is the same layer and also has this loading feature). The light-colored soft sediment deformation bed beneath the dark gray load flow bed is comprised of coarse, bioclastic, packstone-grainstone. The basal bed reveals mound-shape antidunes in laminated beds followed upwards by a bed with apparent internal deformation features (Fig. 5B). The mound-shaped antidunes have a northeast to southwest strike at about 70° (Fig. 5C). The distance between the sinuous wave crests is 30–35 cm, and wave height is about 2–3 cm. It was difficult to determine whether the current was predominantly north-northwestward or south-southeastward. Paleoslope was towards the south-southeast.

The gray colored bed above the antidunes with all the load deformation features in Figure 5B is a coarse to very coarse, massive, packstone-grainstone, which contains abundant poorly sorted corbulid granules and other bioclastic debris. It has a contorted turbulent appearance like the underlying light-colored soft sediment deformation bed in Figure 5A, which was a liquified carbonate sand during emplacement. Joints or cracks in the bed mostly strike from 40 to 70°, but some individual load-flow structures broke away in various polygon forms (Figs. 5A and 6A). Overall, this bed is interpreted as a debris flow, specifically after the manner of a highly concentrated mixture with low mud content (Marr et al., 2001).

With coherent debris flow mixes by weight of 1.5–3% bentonite (fines for mud), 25–30% water, 62–68.5% fine sand, and 5% coal slag (to represent scattered clasts), the features that Marr et al. (2001) produced are identical to this basal bed at Big Josh-

Figure 3. *Corbula* bed at Middle Creek Roadcut. (A) The shoes of the person are standing on the hard, ledge-forming, iron-stained *Corbula* bed. The top surface is rough but relatively flat when compared to its sharp, erosional, undulating contact (often repetitive concave up) with the underlying *Orbitulina texana* bearing packstone. (B) Close-up of the contact of the dark iron-stained *Corbula* bed overlying the lighter gray packstone. The cause of sole marks includes unequal loading and currents.

ua Creek shown in Figures 5 and 6. The low amount of fines causes the flow to behave more like a plastic and its transformation increases at higher velocities (Marr et al., 2001). The soft sediment deformation structures beneath these blocks in Figures 5A and 6A could be referred to as load waves rather than load casts because loading from the overlying denser bed caused them to form (Sullwold, 1959, 1960; Holland, 1960). However, when the underlying material is sand that was liquified in association with debris flows, they are often called water-escape structures and sand volcanoes (Johns et al., 1981; Molina et al., 1998; Marr et al., 2001).

As Figure 6B shows, there is an even darker bed, nearly black, that occurs above the debris flow bed. A comparison with Figures 3 and 4 shows this to be the ubiquitous hard iron-stained *Corbula* bed, which averages about 15 cm in thickness in this area. It has a sharp contact with the underlying bed and a turbulent appearance. On the downthrown side of a small fault, the rolling waters of the creek have exposed iron-stained asymmetrical antidunes in this bed that strike at 150°. The distance between wave crests is about 56 cm, and wave height is at least 3 cm (Fig. 6C). Flow direction is clearly towards the northeast, +/- 60°. The small fault, with less than a meter of displacement, crosscuts overlying strata and occurred after deposition of the *Corbula* sequence. The fault has a strike of about 65°.

At Canyon Lake Gorge, the lower half of the *Corbula* sequence contains a succession of three medium-very coarse packstone beds, which are illustrated in Figure 2. The lowest bed contains lunate bedforms that strike at about 10° with a westward flow direction of 280° (Fig. 7). The distance between wave crests is 30–40 cm, and wave height is about 4–5 cm. Lunate bedforms are related to linguoid forms, which indicate high velocity and decreasing flow depths (Twenhofel, 1932; Selley, 1988). They are known to occur in conjunction with antidunes caused by tsunamis (e.g., Smit et al., 1994). They appear to collide with mound-shape antidune wave crests that strike east-west, thus paleocurrents were north-south (Fig. 8). Overriding these beds is the top bed, which contains a variety of ripple forms on the surface (Fig. 9). As seen in Figure 9, the paleocurrent can be ascertained because the smooth light-colored stoss side is visible along with mini avalanches of corbulids on the down-current lee side. Remnants of the smooth stoss side occur in other dune-shape bedforms, but most of these structures collapsed as indicated, which is typical of antidunes if current direction changes and/or velocity is reduced (Middleton, 1965; Skipper, 1971). The paleocurrent moving northeastward was rotated towards the north. This upper surface of the lower half of the *Corbula* sequence correlates well with surficial antidune bed at Big Joshua Creek shown in Figure 6C. The basal beds correlate with the debris flow bed of Figures 5 and 6 because a more-or-less north-south paleocurrent evidenced by antidunes occurs at both locations.

The Blanco River section has excellent exposures of the *Corbula* sequence in the cliffs adjacent to the river. Instead of the typical dark gray color with deep orange-red iron staining, the bed is buff colored with light iron staining. The corbulids occur as naturally polished steinkerns in pristine condition as river or spring water have cascaded over the bed (Fig. 10A). The site is located about 100 m upstream of a low crossing bridge along Highway 1623 about 5.3 km west of the town of Blanco. At this location, the *Corbula* sequence was deposited upon a medium-dark gray limy mudstone, which also contains coarser tan lenses of carbonate debris. It looks like shale, but a quick test demonstrates this rock readily fizzes with dilute HCl (Fig. 10B). As Figure 2 indicates, this mudstone (to the naked eye) is a fine-

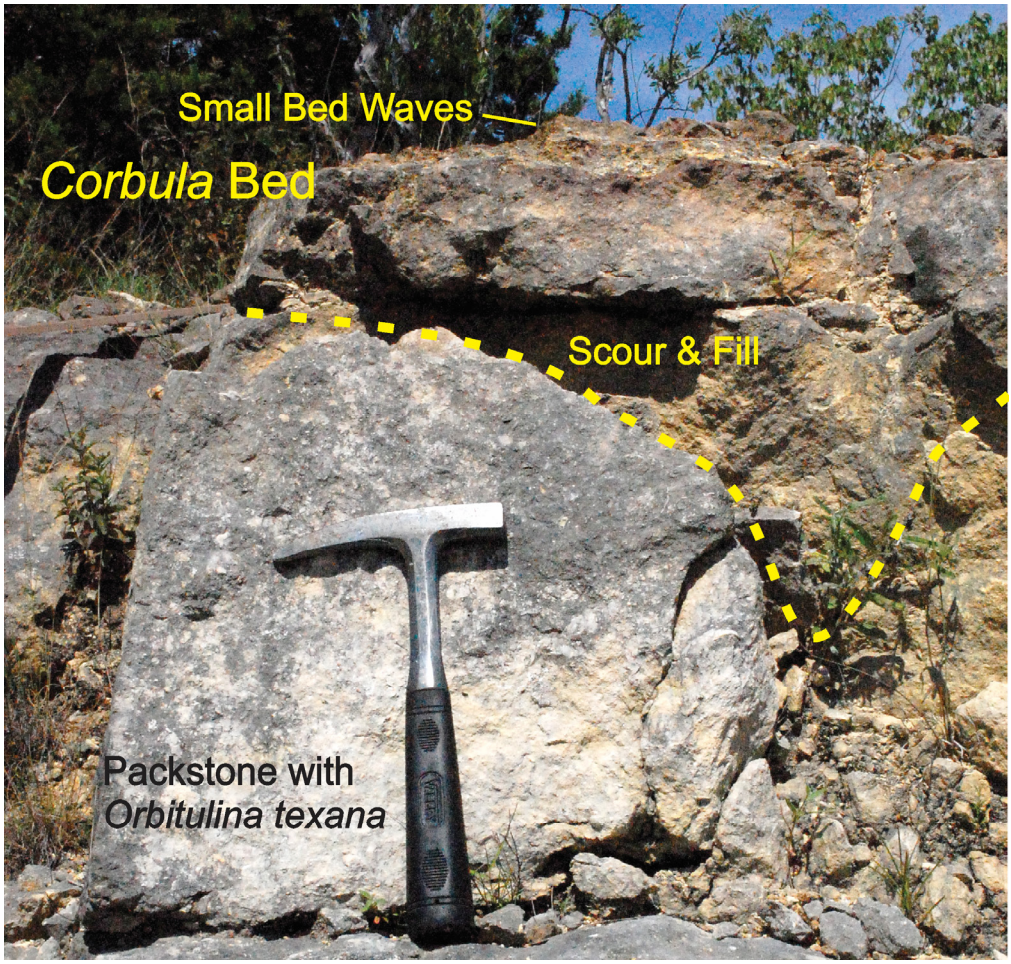

Figure 4. Sedimentary structures in the *Corbula* bed at Middle Creek Roadcut. Deep erosional scour and load features cause rapid changes in bed thickness. Small, three-dimensional bed waves, linguoidal, occur on the surface. Strike ranges from 155–180°, and the steeper lee side is towards the east-northeast.

grained packstone with ostracods and miliolids. The contact of the overlying *Corbula* bed with the mudstone is sharp, erosive and undulating. In Figure 10B, the first plane beds appear slightly wavy or hummocky with additional sharp contacts between. Then a rather large lenticular hummock occurs and from this vantage point is about 50–60 cm long (the hammer is roughly 28 cm in length). When observed from the ledge, the large hummock is a mound-shape antidune (Fig. 10C). Two of these occur side by side. The strike of the wave crests is again 150°. The distance between wave crests is about 45 cm, and wave height is a little more than 4 cm. As seen in Figure 10A, the elongate corbulid shells align northeast-southwest.

The alignment of the steinkerns appears perpendicular to the strike, but the more-or-less mound shape made it difficult to determine whether the paleocurrent was northeast or southwest. Observations of the corbulids, here and at Canyon Lake Gorge also align themselves somewhat perpendicular to the strike of the wave crests. In prior studies of elongate shells, it was noted that *Turritella* shells aligned perfect current-parallel with the pointy thinner apex end up-current (Brenchley and Newall, 1970). As seen in Figure 10A, the pointy posteriors point in two primary directions, northeast and southwest. The corbulids elongate shape was analyzed in a hand sample to learn if the broad anterior or thinner posterior end made any difference with alignment. Out of a count of 65 corbulids in a 9 cm^2 area, the anterior end of 21 corbulids pointed in the 60–90° range while 20 pointed in the opposite direction from 240–270°. This pattern indicates that the elongate shape of most corbulids do align somewhat parallel to the flow (i.e., perpendicular to the wave crests). But the pointy posterior of corbulids in this birds-eye view could only narrow the paleocurrent to be either southwest or northeast, since an equal number of shells pointed in each of the opposing directions.

Figure 10C also shows wavy plane beds, which thin upwards. Polished slabs of some of these thin beds contain imbricated corbulids and small flame structures that indicate a northeasterly flow followed by a southwesterly flow. The scattered pattern of corbulids, in a more-muddy matrix, is similar in appearance to the sample gathered and examined from the Williams Creek site, Bandera County. Stricklin et al. (1971) believed that this was due to the fines being winnowed from the east and transported to the western part of the shelf. Above the wavy thin beds is a soft, crudely bedded wackestone-packstone, which is capped by a waving packstone with abundant ostracods, which is viewable in Figure 10B and shown in Figure 2. This soft friable bed contains a lot of sand-size particles and marine megafossils. In Figure 2, this wackestone-packstone bed is also described from observations at Canyon Lake Gorge and Big Joshua Creek. The only difference is that the wavy packstone that caps the soft friable wackestone does contain corbulids at these two locations. At Canyon Lake Gorge, another wavy thin bed within the crudely laminated wackestone is about 1–2 cm thick and contains abundant corbulids, a few *Orbitulina texana* fossils and other shell debris.

The substrate upon which the *Corbula* bed was deposited varies. At some places it was rather hard while at other places the substrate was soft and unlithified. A few borings were seen below the *Corbula* bed at Twin Sisters roadcut and in a localized area just beneath the basal bed of the *Corbula* sequence at Canyon Lake Gorge shown in Figure 7. The nested borings, in a stratum about 15 cm thick, range from about 1–2 cm in diameter. They are much larger than what a granule-sized clam would

Figure 5. Lowest bed of the *Corbula* sequence at Big Joshua Creek has antidunes overridden by a debris flow. (A) The dark gray bed in the foreground and background is the debris flow, a massive, coarse packstone with poorly sorted corbulids. The load-flow structures (foreground) are jointed with a concave up sharp contact. Differential loading on a liquified coarse carbonate sand caused load waves or sand volcanoes to rise, which deformed the debris flow bed even more. (B) Closeup of the dark gray debris flow above antidunes. Note the internal, turbulent, contorted deformation of the bed. Its character is like the soft sediment deformation bed in (A). (C) Antidunes strike at about 70°.

make. This bed at Canyon Lake Gorge is considered a subtidal hardground where these occur (Ward and Ward, 2007). Many of the tunnels are more-or-less horizontal, but a couple vertical ones penetrate the westward flowing antidune and may represent escape structures as the organism crawls upward to reach the surface before burial by great quantities of sediment (Häntzschel and Frey, 1978). No other borings were seen in the *Corbula* sequence, even in the finer, muddier soft friable sediments that overlie the supercritical flow bedforms.

Antidune Analysis

The structures in the lower half of the *Corbula* sequence are antidunes for several reasons. First, there is the mound shape (Middleton, 1978; Allen, 1982a; Barwis and Hayes, 1985; Selley, 1988; Rust and Gibling, 1990). Secondly, the distance between the mounds of wave crests along with wave heights line up with other flume and field studies (Table 2). The wavelengths of 30–60 cm and wave heights of 2–5 cm, typical for the *Corbula* bed, align well with the previous studies in Table 2, especially those with medium to very coarse particles (Skipper, 1971; Yagishita and Taira, 1989; Rust and Gibling, 1990). The only outlier, with smaller wave heights, is the study by Hand (1974) who used pulverized charcoal to mimic an erodible bed. The variability seen in Figures 5–10 occurs because antidunes in nature are three-dimensional structures (Allen, 1982a; Rust and Gibling, 1990; Alexander et al., 2001). The primary structure is a concave-up erosional trough in which lamina dip up-current or fill the troughs symmetrically, and constant reworking of sediment leads to asymmetrical forms in which erosive downdip lamina occur (Alexander et al., 2001). Thirdly, and most important of all, it was vital to examine the sedimentary structures within a corbulid antidune.

The mound-shapes are observed to be slightly asymmetrical with a longer stoss side and shorter lee side (Fig. 11). Figure 11A is an outcrop photograph from the same bed with the lunate bedforms in Figure 7 at Canyon Lake Gorge. The view is northward and perpendicular to the strike of the waveform. The elongate corbulids align east-west across the top of the bedform. Figure 11B is a sample from the Blanco River site shown in outcrop of Figure 10. This sample was cut perpendicular to the wave crest and polished. The angle of the front side of both bedforms if Figure 11 dips upcurrent and has a nose-like structure pointing downcurrent. A close examination of Figure 11B reveals low-angle cross-beds in the bottom of the structure that dip upcurrent. This is better seen in the zoomed image of the same sample in Figure 12.

Figure 12 shows low-angle cross-beds in the bottom portion of the sample that are sometimes called backset beds as they dip upstream (Allen, 1982a; Barwis and Hayes, 1985). The central dark area, which can also be seen in Figures 11A and 11B, is where finer material accumulates. The outline of several corbulid steinkerns was done to demonstrate the imbrication pattern of these particles. Most of the tear-drop shape corbulids in the low-angle backset beds and across the upper 1 cm of the bedform dip to the left resembling shingles. The dip direction is up current meaning they tilt or lean in the downflow direction because they are tipped over by the flow. The imbrication pattern is a good

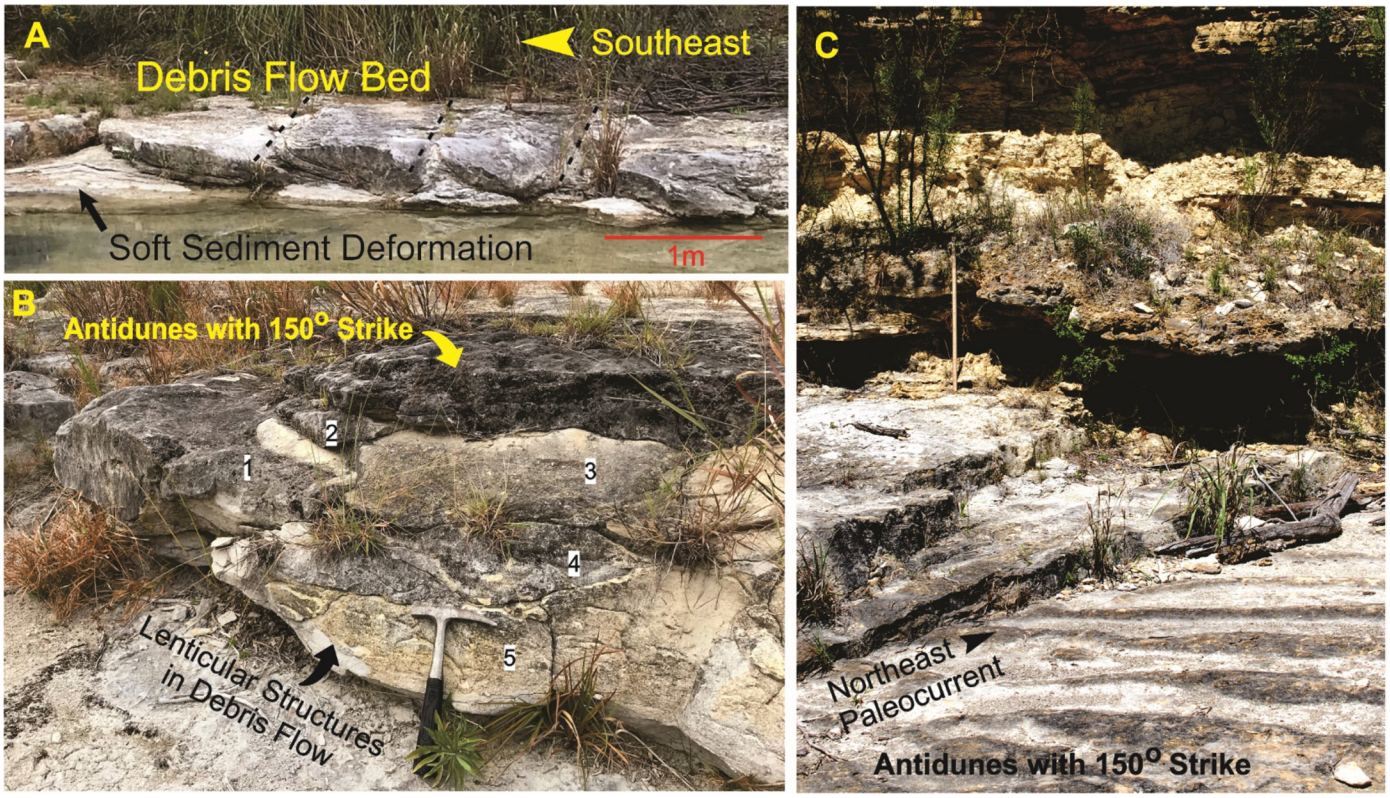

Figure 6. Debris flow at Big Joshua Creek with lenticular structures and overriding antidune bed. (A) Individual lenticular pieces of the debris flow with transverse cracks. Most of the joints strike from 40–70° (dashed lines); the dip of individual pieces is to the northwest. Flow was towards the southeast. As the debris flow came to rest, detached pieces in arrears slid atop those in front in an imbricated collision pattern aided by the liquified carbonate sand beneath. (B) The plasticity of the debris flow with low mud content caused a large variety of lenticular structures (1–5) to form by a combination of flow, loading, and sliding. Lenticular structure #1 slid up the back of 4 and 5 and pierced 3. In appearance, #2 and 4 are nearly perfect lens shapes with a concave-up base and convex-up or hummocky surface. Lens #2 may be a transitional bedform between the debris flow and overlying dark gray antidune bed. (C) A small fault with a strike of about 65° and a throw of less than a meter (see meter stick leaning on the cliff) occurs in the area. The northeast-southwest fault trend is common in the region (Fig. 1). Erosion of the rolling waters of the creek has exposed the asymmetrical antidunes on the downthrown side. The wavelength and wave height are about 56 cm and 3 cm respectively, and paleocurrent was towards the northeast at about 60°.

match of elongated particles used in antidune flume experiments (Yagishita and Taira, 1989). In that study, Yagishita and Taira (1989) demonstrated that elongate particles tilt away from the direction of motion and imbrication is preserved on both sides of the antidune. The laminations shown by dashed lines of the upper 1 cm surface dip down current. The basic pattern to make these antidunes is a scour-and-fill process that Allen (1982a, his page 414 and figures 10–2) sketches out in his book, with just a slight variation with regards to the central swelling of the bedform, as follows. The trough is eroded and quickly followed by deposition as low-angle upstream dipping cross-beds across the bottom while finer particles are winnowed and caught up into the central vortex. In the central vortex, the finer particles circulate upwards and in reverse flow as seen in a few imbricated corbulids that were caught up along with the fines in the center. This is evident in Figure 12A and sketched in Figure 12B. This process swells the bedform with predominantly finer particles in the center as the larger corbulids were lifted higher in the flow and redistributed across the upper part of the structure. The flow continues to deposit the coarse elongated corbulids, by tilting them downstream (i.e., particle dip is upstream) and placing them in sets of downstream-dipping current lamina. Thus, antidunes grow by erosion of the troughs and deposition on the crests (Alexander et al., 2001).

Antidunes form in supercritical flows (Alexander et al., 2001; Cartigny et al., 2014). The velocities needed in the formation of corbulid antidunes, which is comprised of a medium-very coarse carbonate sand, can be roughly estimated from fluvial studies. The specific gravity of carbonate sands is about the same as quartz (Twenhofel, 1932). Hjulström's diagram indicates that the velocities needed to pick-up granules (2–4 mm), which represents the mean diameter of larger corbulids, is between 1.6–1.8 m/s (Thornton, 1978). Antidunes have formed at corresponding velocities during storms in fine sand washover fans with mean overwash velocities from more than 1.5 m/s to more than 1.9 m/s (Barwis and Hayes, 1985). Thus, it seems safe to say that the corbulid antidunes, with much coarser granules, must have formed from seafloor erosive velocities of at least 1.5 m/s, but more likely approaching 2 m/s. Granules fall out of suspension and deposit when velocities reduce to 1.1–1.4 m/s (Thornton, 1978).

Antidunes are known to form in rivers, storm washover fans and on beaches such as drainage channels and intertidal backwash (Allen, 1982a; Alexander, 2001). Because these are all shallow water environments, antidune wavelengths have been used to estimate shallow flow depths. Coastal swash and backwash studies in fine sand have produced high speed flows up to 1.5 m/s in water depths up to 6 cm (Allen, 1982a). In medium sand with a mean flow velocity of 1.4 m/s, a great variety of three-dimensional antidune bedforms were generated as the initial flow depth of 7 cm became 2–3x greater due to hydraulic jumping (Alexander et al., 2001). It has also been known for

Figure 7. Lowest antidune bed at Canyon Lake Gorge. Several lunate wave crests occur with steeper lee sides facing west, therefore flow was towards the west (e.g., Leeder, 1982). The strike of wave crests is roughly 10° so paleocurrent moved at +/- 280°. Other more mound-shaped antidunes (lower left and upper part of the photograph) are slightly asymmetrical with a longer, gentler stoss side to the east and steeper lee side to the west. Distance between wave crests varies between 30–40 cm with wave heights of 4–5 cm.

some time that antidunes form in turbidity currents and density underflows in deeper water environments (Skipper, 1971; Hand, 1974; Allen, 1982a; Alexander et al., 2001; Cartigny et al., 2014). Lastly, and of utmost import to this study is that tsunamis produce antidunes (Fujiwara, 2008; Keating et al., 2008; Shiki et al., 2008b; Sugawara et al., 2008; Phantuwongraj and Choowong, 2012). Velocity and turbulence along the seabed matter more than water depth.

Thin Section Analysis

Photomicrographs of the polished antidune sample from the Blanco River site in Figure 12 further illustrate the rapid circulatory processes involved in corbulid antidune formation (Fig. 13). Ostracods, miliolids, and peloids dominate the fine fraction in central vortex. These constituents dominate the gray mudstone bed that underlies the *Corbula* antidune bed shown in Figure 10. There is little doubt that these particles came from that bed. The abundance of ostracods and miliolids beneath the *Corbula* bed in this local area could suggest hypersaline conditions (e.g., Nagle, 1968). The corbulid shells occur in a packstone cemented by biosparite (Fig. 13C). Infilling of corbulid shells differs. Some shells are filled with peloids, others with bladed to blocky calcite cement, and yet others with miliolids, peloids, and some calcite cement. The outline of shells is intact. It is certain that the corbulids are allochthonous and were transported and buried in a high energy environment. Corbulids prefer living in fine-grained sediments from the intertidal zone down to 50–100 m water depths where they place their posterior upwards in more-or-less vertical position of shallow burrows (Lewy and Samtleben, 1979). Corbulids could tolerate hypersaline conditions (Nagle, 1968; Stricklin et al., 1971). However, they have a low tolerance for waves and currents (Lewy and Samtleben, 1979).

When swept up by such processes, corbulids close their inequivalve shells air-tight, but after death, decomposition of the MCL (main conchiolin layer) causes each valve to separate into two shells (Lewy and Samtleben, 1979). The shell will not separate when they are buried rapidly (Försich and Pan, 2016). Because no burrows have been observed and the bivalves are articulated in the *Corbula* sequence indicate that the corbulids were transported alive (Scott, 2007; Försich and Pan, 2016). Once buried and suffocated the shells initially contain little to no sediment but fossilize by diagenesis processes after the event (Försich and Pan, 2016). Under the normal, everyday life and death of organisms, it is possible that some corbulids recently died within the burrows and were initially filled with some debris. Subsequently, they were eroded shortly after death and reworked into the antidunes as bioclastic allochthonous debris. The burrows themselves and the environment in which they lived were completely obliterated. The corbulids do not exist in underlying sediments anywhere in the study area, except in the *Salenia* beds to the far southwest in Bandera County. This means that

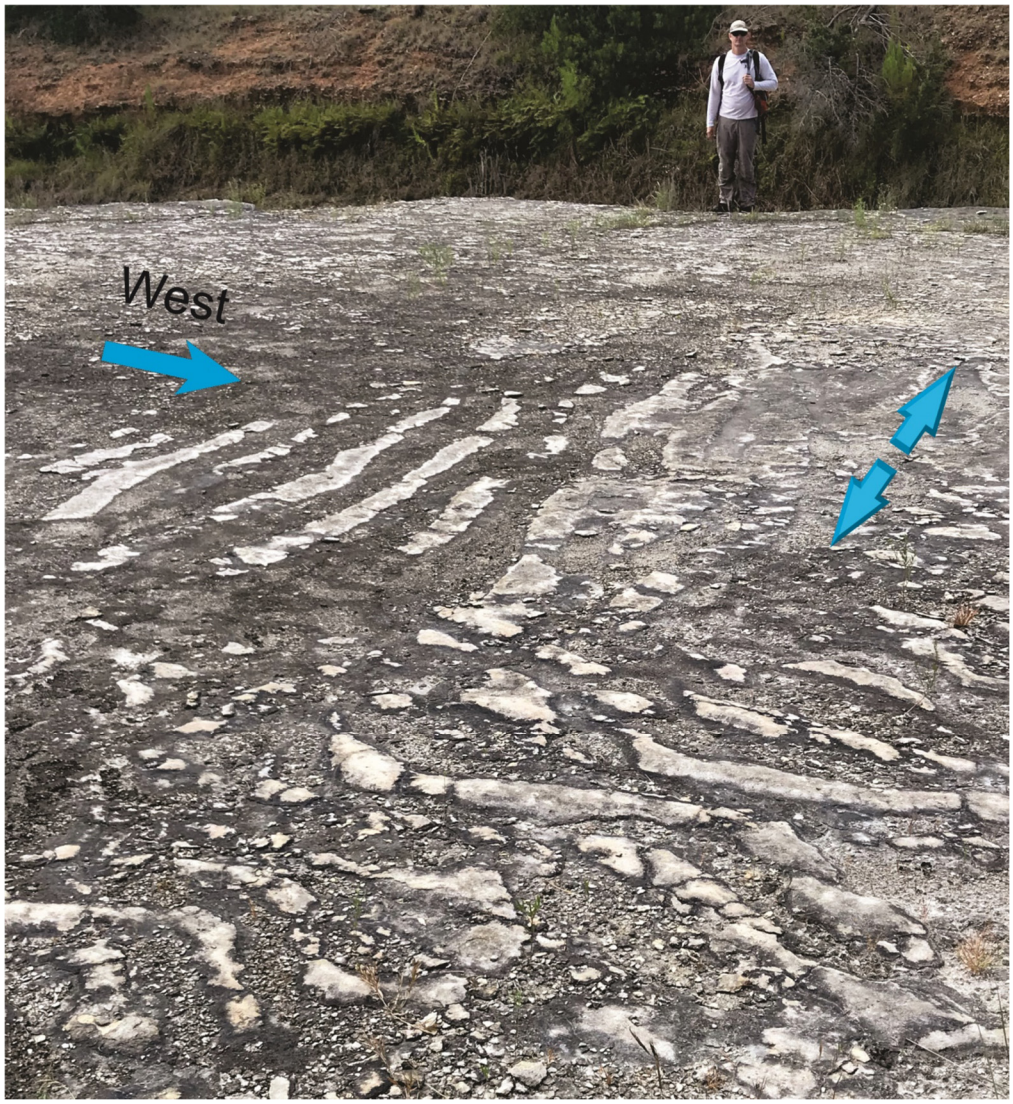

Figure 8. Lower to middle antidune bed at Canyon Lake Gorge. The westward moving paleocurrent appears to collide with the north-south wave crest pattern on the right side of the photograph. View is towards the southeast. Flow to the west (see also Figure 7) and south may have been caused by tsunami drawdown. The flow back to the north seems to have been quite strong. The northward flowing current caused the current of the surficial antidune bed to rotate at least 45°.

living or dead, these bioclasts were all eroded from their previous living environment across the large region and reworked into catastrophic high velocity structures. Unbroken and unabraded shells are common in tsunami deposits (Shiki et al., 2008b). It is not known exactly how far the corbulids were moved nor how long they remained suspended in the turbulent flow. But their shells did not break apart during transportation nor after deposition, which indicates rapid burial (Försich and Pan, 2016).

Besides Blanco River, photomicrographs of the lower half of the *Corbula* sequence also testify of a high energy environment at the other locations (Fig. 14). At Canyon Lake Gorge a sample was gathered from between wave crests of the surficial bed seen in Figure 9. It shows imbricated corbulids with finer particulates above (Fig. 14A). This indicates that some finer material accumulated in the troughs between corbulid wave crests. Corbulids are filled with carbonate cement including peloids and miliolids. Some locations have an abundance of debris other than corbulids (Figs. 14B–14D). At the Little Blanco River, the iron-stained bed contains an abundance of miliolids, fossiliferous algae, peloids and few corbulids (Fig. 14B). The lack of mud indicates high energy. The same occurs at Middle Creek roadcut previously shown in Figures 3 and 4. There are rare if any corbulids and a lack of mud (Fig. 14C). The bed is rich with *Orbitulina texana*, miliolids, and other fragments in an environment so energetic that some *Orbitulina* were left suspended in an unnatural edgewise, more-or-less vertical position. The iron-stained *Corbula* bed at Twin Sisters roadcut is badly weathered. A few borings and *Orbitulina texana* fossils were seen below the *Corbula* sequence. However, just above the iron-stained stratum is a thin gray in-situ hard mudstone 1–1.5 cm in thickness. In outcrop, this mudstone looks like the ostracod-miliolid mudstone beneath the *Corbula* bed at the Blanco River site shown in Figure 10. In thin section, miliolids and peloids are the most common grain type (Fig. 14D). Ostracods are either rare or nonexistent in this mudstone. The silt sized miliolids and peloids and little mud classifies this as a fine grained packstone. Perkins (1974) exaggerated the thickness on his section and called it a calcareous shale, which he placed in the middle of a corbulid rich wackestone. Thin mud seams like this have been noted in tsunami deposits between waves (Peters and Jaffe, 2010). The calmer interval for this mud deposition takes only tens of minutes or no more than an hour (Fujiwara, 2008; Sugawara et al., 2008).

DISCUSSION

The key features of this study are displayed on a very generalized paleogeographic map (Fig. 15). Antidunes occur in the type *Corbula* bed, which corresponds to the lower half of the *Corbula* sequence of Figure 2. They were seen at 5 of the outcrops, but the flow direction could not be obtained at Golds Road, Hays County. The lower antidune beds have a north-south component, specifically the wave crest strike at Big Joshua Creek

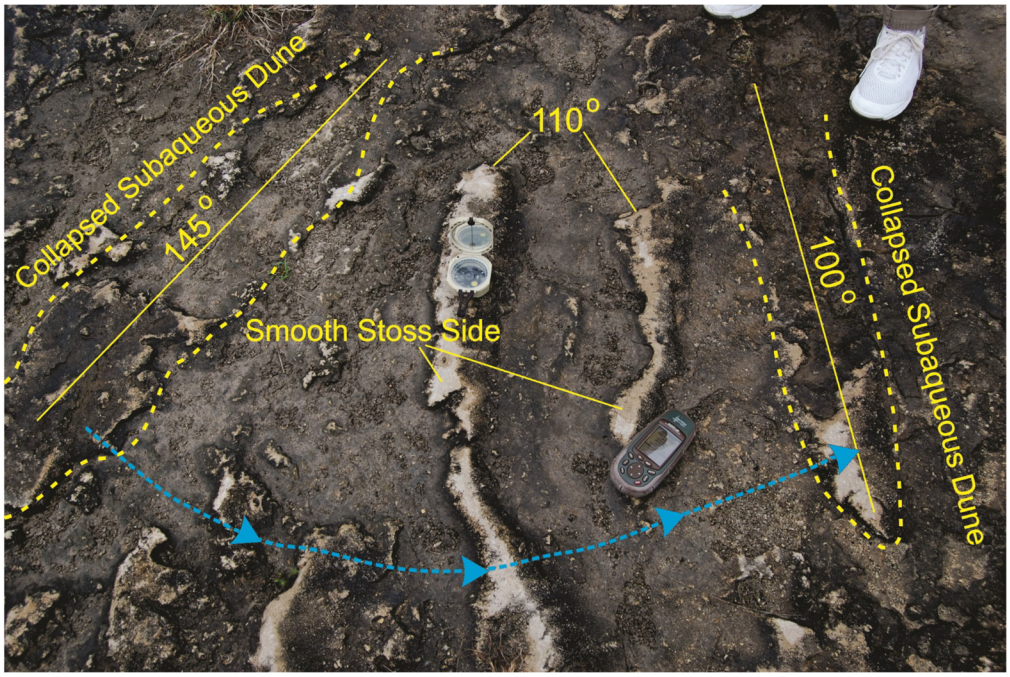

Figure 9. Uppermost antidune bed surface at Canyon Lake Gorge. The light color on these bedforms is the smooth stoss side of the various subaqueous dunes. The bedforms are slightly asymmetrical with small fans of corbulid avalanches on the lee sides (see right of Brunton compass), which indicates current direction (e.g., Leeder, 1982). A remnant of the light-colored stoss side is evident on the dune with a strike of 100°. The rest of the structure has collapsed, which can also be seen in the structure that strikes 145° and others towards the bottom of the photograph. The multiple strike pattern of these bedforms indicates a counter-clockwise rotation (blue arrow) pattern indicative of eddies or whirlpools. When velocity decreases, antidunes are known to collapse (e.g., Middleton, 1965). The spacing between wave crests is as close as 30 cm, but increases to about 50 cm.

in Kendall County is about 70° and the strike at Canyon Lake Gorge at 100°, previously indicated in Figure 5C and Figure 9. The antidunes that moved practically due west were only observed at Canyon Lake Gorge, Comal County; recall Figures 7 and 8. Overriding the lower antidune beds are those with a strike of 145–150°, paleocurrent direction of about 60°. These northeast flowing antidunes occur at Big Joshua Creek, Canyon Lake Gorge, and the Blanco River site previously displayed in Figures 6, 9, and 10. At Hamilton Creek, Travis County, the wavelengths up to 60 cm occur along with wave heights of 4–5 cm. The strike of the slightly asymmetrical mounds is +/- 120° and flow was towards the northeast about 30°. All antidune beds occur in quick succession, there are no borings, and not a single corbulid could be observed in life position. Instead, they occur as reworked bioclasts in antidunes, a supercritical flow structure.

Tides and Storms

The *Corbula* bed in this study area was considered an intertidal deposit (Stricklin et al., 1971). But the velocity of normal tidal currents is on the order of a few centimeters per second (Garrison and Ellis, 2016). This is well below the supercritical velocities needed to form antidunes. Some studies do show antidunes in the intertidal zone along the shore of the Bay of Bengal at the town of Digha (Chakrabarti, 2005). These antidunes look like the ones at Canyon Lake Gorge in Figure 8. At Digha, the tidal flat experiences a strong swash and backwash pattern due to short period waves during the summer and monsoon months; wind speed averages 46 km/hr, while cyclonic wind speeds reach 74–93 km/hr (Chakrabarti, 2005). The Digha antidunes have about the same wavelength as Canyon Lake Gorge, but the smaller sand size of roughly 0.3 mm is much finer than the *Corbula* antidunes, thus lower seafloor velocities would be needed to rework fine sand. Nevertheless, it does demonstrate that storm driven tides with high-velocity winds in shallow water can produce antidunes. Tide velocities also increase through narrow passageways and form tidal bores; some move at 3 m/s (Garrison and Ellis, 2016). But the geomorphology does not fit descriptions of this extraordinarily wide relatively flat lagoon where the *Corbula* bed was deposited (e.g., Perkins, 1974). Thus, normal tides could not have formed the antidunes of the *Corbula* bed. Tsunamis cause swash and backwash (Coleman, 1978; Sugawara et al., 2008). Besides this megaripples with wavelengths of 1 m diminishing inland to 20 cm with the wavecrests in the form of concentric semicircles open to the sea look like concentric forms in Figure 8. These were formed by the 2004 Indian Ocean tsunami from very coarse sand that was scoured 60 cm in depth (Goto et al., 2008). A tide by itself cannot make antidunes in a lagoon.

Distinguishing between deposits caused by large storms and tsunamis is quite difficult because the hydrodynamics is similar (Shanmugan, 2006; Bourgeois, 2009; Phantuwongraj and Choowong, 2012). The lagoon in Central Texas was rather flat, the regional slope of the *Corbula* bed when deposited was less than 0.05° towards the south-southeast (Stricklin et al., 1971, their figure 11). Closer to the Llano islands in the adjacent Hensel Sand (also called Gillespie Sand) facies that lapped the islands' land surface, the depositional slope increased to about 0.33° (Stricklin et al., 1971). This suggests a normal runoff from the islands southward into the sea. Based on the regional slope, flood tide was to the north-northwest and ebb tide to the south-southeast. Therefore, the north-south trend of the lower antidune bed displayed in Figures 5, 8, and 15, could be an indicator for accelerated processes in the same general directions as the rise and fall of tides. For example, major storms induce a combination of unidirectional and oscillatory currents, which move enormous amounts of sediment (Shanmugan, 2006). Category 5 Hurricane Ivan generated waves 27 m high and accelerated currents on the shelf bottom to exceed of 2 m/s in 60–90 m of water (Shanmugan, 2006). In shallower depths approaching the lagoon setting, 5 m/s are estimated near the bottom in 20 m water depths, in which even gravel size material would be eroded, transported, and deposited elsewhere (Shanmugan, 2006). Like tsunamis, storms also have the power to deeply erode seabed sediments. Direct measurements on shelves indicate erosion 1–2 m deep (Shanmugan, 2006). At these flow velocities and erosive capabilities, corbulid granules could easily be reworked by storms.

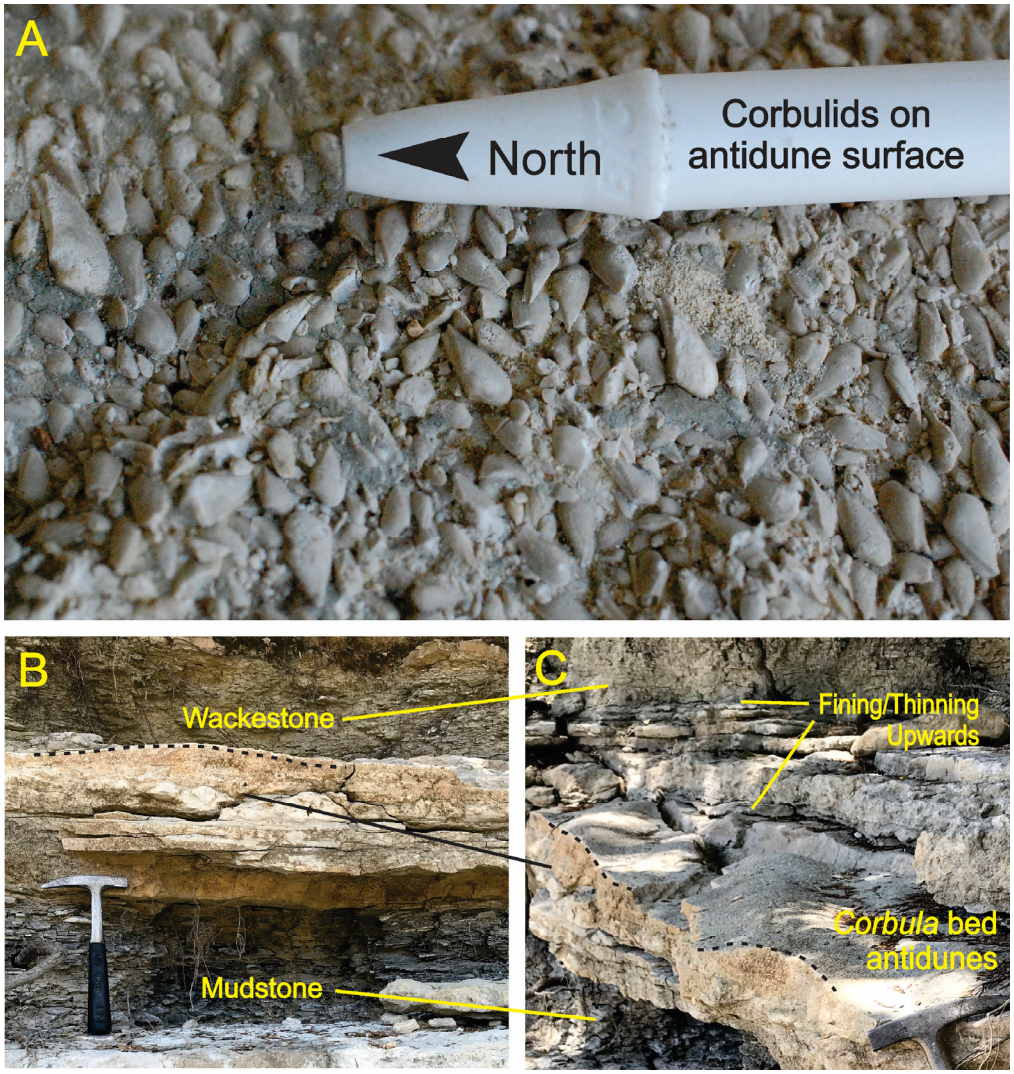

Figure 10. Blanco River locality. (A) Surface of the *Corbula* antidune bed shows that many corbulid shells align northeast-southwest, which is perpendicular to the wave crest strike of 150°. (B) The contact of the antidune bed with the underlying gray mudstone is sharp and gently concave up. The dashed line is convex up and represents a hummock at the top. The beds in between are typical three-dimensional antidune features (e.g., Alexander et al., 2001). The view is towards the north. (C) The dashed lines represent two hummocks or mounds. The black line points from the same approximate spot from image (B). The two mounds are antidunes that strike at 150°. The distance between wave crests is 45 cm, and the wave height is about 4 cm. Superimposed on the antidunes are wavy plane beds that fine and thin upwards. This is followed by a friable wackestone, which is also shown in (B).

However, the creation of antidunes caused by storms seems limited to small geographical areas such as the tidal flat in Digha and storm washover fans (Barwis and Hayes, 1985; Chakrabarti, 2005). One of the largest storm washover fans measured 6 km in diameter (Barwis and Hayes, 1985). This equates to an area of 38 km^2. In Figure 15, it can be ascertained that antidunes in the *Corbula* bed cover at least 4000 km^2.

Storm deposits and those caused by the 2004 Sumatra-Andaman tsunami were compared in Thailand (Phantuwongraj and Choowong, 2012). In this study, the researchers studied the tsunami deposit along the Andaman coast and compared the results with known storm deposits on the east coast of the Gulf of Thailand. The primary difference between the two types is that antidunes occur in the lower part of the tsunami deposit and do not occur in any of the storm deposits. Moreover, ripples and other dunes formed on the surface of tsunami antidune beds, and rip-up clasts were more abundant, but rare in storm deposits (Phantuwongraj and Choowong, 2012). To account for this, they suggest that storms may not have the same velocity as tsunamis. As shown earlier, this cannot be the main reason (e.g., Shanmugan, 2006). Antidunes are formed when there is a high concentration of suspended sediments; and are preserved either by rapid deposition or diversion of the current (Skipper, 1971; Yagishita and Tiara, 1989). The *Corbula* sequence contains evidence that both processes played a significant role. On shallow shelves, storms, even storm surges, tend to deposit graded sand beds, plane beds, planar laminations, and hummocky cross-stratification (HCS) (Nelson, 1981; Dott and Bourgeois, 1982). The preservation of antidunes at a scale of thousands of square kilometers requires the energy of a tsunami because once flow is reduced antidunes flatten into plane beds (Middleton, 1965; Skipper, 1971). Therefore, it seems that the waning stage of storm driven currents differs somehow in velocity and suspension processes. A single tsunami is known to affect hundreds of kilometers along coastlines (Bryant and Knott, 2001). This fact along with the presence of antidunes across the platform over such a large area is indicative of a tsunami.

The Debris Flow

The debris flow with soft sediment deformation structures, seen only at Big Joshua Creek, may be a local feature of the basal *Corbula* bed in this area. The overall size is not known. It can be traced across the creek in both directions where it disappears beneath other strata on each side of the creek, which is no more than 50 m wide. The length was not measured because it has been eroded away downstream. The debris flow bed moved southeast down a paleoslope of less than 0.05°. One way to cause a debris flow in shallow water is at the front of alluvial fan deltas that prograde into seas from adjacent highlands (Postma, 1984). There very well could have been a prograding delta within the Hensel Sand that emanated southward from the Llano island(s). The cross-section in Stricklin et al. (1971, their figure 11) shows that the *Corbula* bed disappears into the Hensel Sand

Table 2. Comparison of antidune wavelengths and heights.

Study	Type	Grain Size or Type (mean)	Wavelength (cm)	Height* (cm)
Middleton (1965)	Flume	Fine Sand (0.19 mm)	100–200	5
Hand (1974)	Flume	Medium-Coarse Pulverized Charcoal (< 1 mm)	28	0.7
Yagishita & Taira (1989)	Flume	Medium-Coarse Sand (0.5 mm)	60–70	3
Skipper (1971)	Field Outcrop, Cloridorme Formation, Quebec	Calcareous Wacke Bed, Medium-Very Coarse	48–100	3–7
Barwis & Hayes (1985)	Field Outcrop, Modern Washover Fan	Fine Sand (0.13 mm)	45–60	1–2
Barwis & Hayes (1985)	Field Outcrop, Peninsula Formation, S. Africa	Very Fine Sandstone	60	3–4
Rust & Gibbling (1990)	Field Outcrop, South Bar Formation,	Medium Sandstone (0.3 mm)	50–110	5–10
The Present Study	Field Outcrop, *Corbula* Bed	Packstone-Grainstone equivalent to Medium-Very Coarse Sandstone	30–60	2–5

***Some authors used the term "amplitude" to describe ripple marks or "ripple-mark amplitude," but this term is equivalent to "height" used by others; the better term is ripple height (Allen, 1982; Jackson, 1998).**

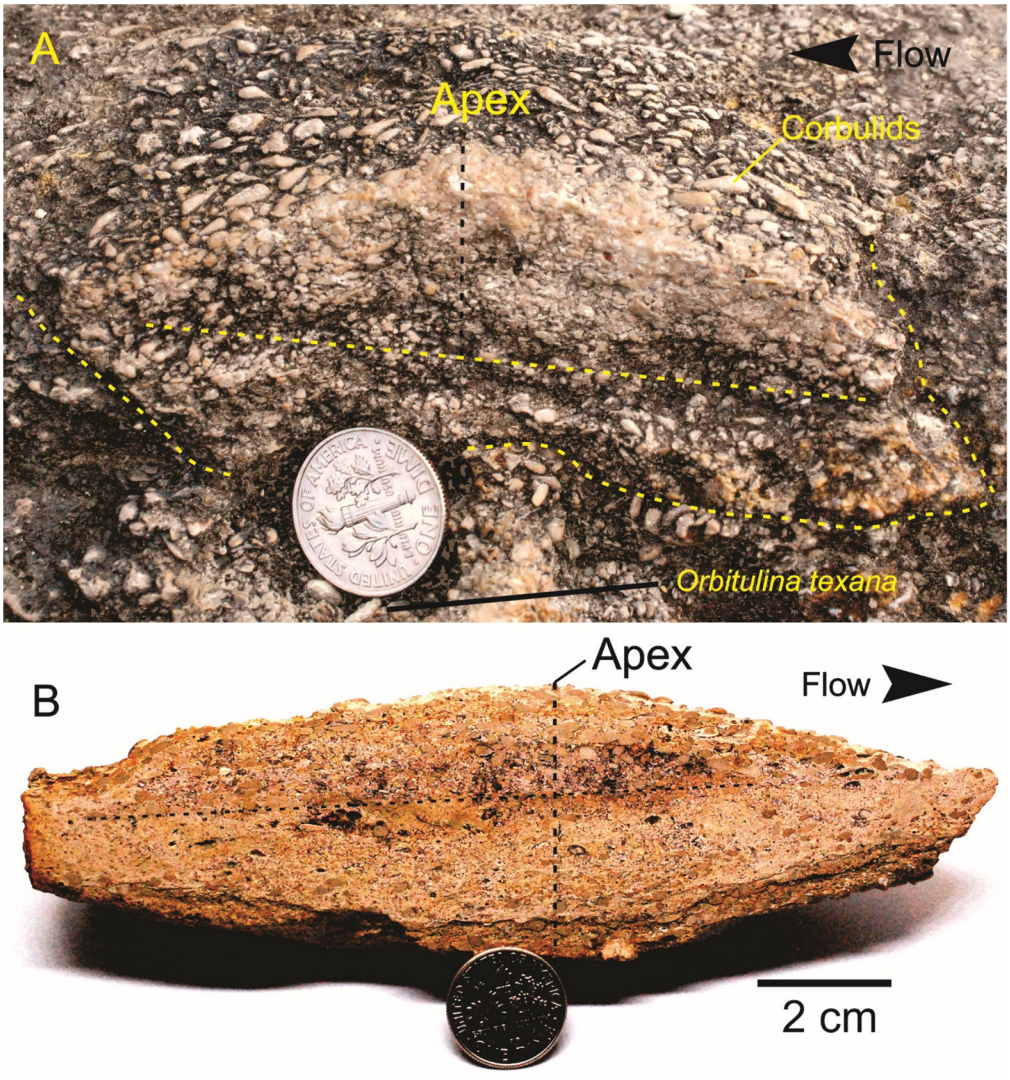

Figure 11. Antidune structure. (A) This sample is from the basal antidune bed at Canyon Lake Gorge. A triangular mound shape is evident at the apex. From the apex the bedform is asymmetrical with a slightly longer, gentler stoss side to the right of the apex and shorter, steeper lee side left of the apex. Paleocurrent was to the left (which is west) and corbulids align parallel to flow direction. The antidune is pointy at both ends. Both, but the leading edge (left) and trailing edge (right), dip upstream with the latter in a zigzag pattern (see yellow dashed line). Similar structures can be found in Alexander et al. (2001, their Figure 5). (B) Polished sample from the Blanco River. It also has a longer, gentler stoss side (left), steeper lee side (right), and the leading edge dips upstream. Flow is towards the right (northeast). The internal structures include gently upstream dipping cross-beds in the lower portion, continuous swelling over the central vortex, and downstream dipping beds. This matches the antidune pattern of Allen (1982, his figures 10–21).

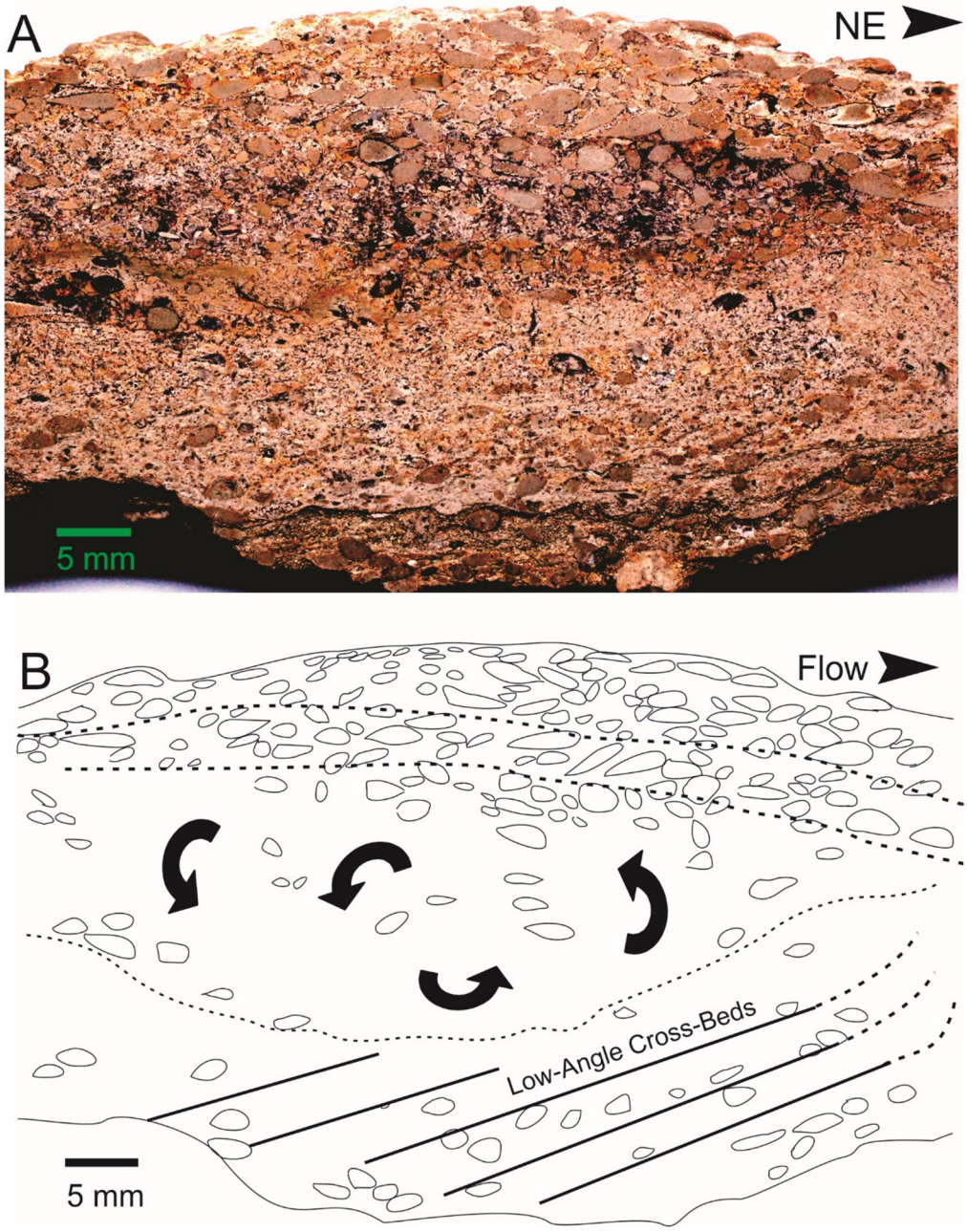

Figure 12. Macrophotography and interpretation of Blanco River antidune anatomy. (A) Closeup of the central portion of Figure 11B, which shows low angel cross-beds along the bottom and imbricated corbulids. (B) Sketch of the image in (A). Faint cross-bedding or laminae gently dip upstream. Because most of the corbulids dip upstream, flow was towards the right, which is northeast. In the center a vortex formed with a counterclockwise rotation as indicated by the arrows. This caused swelling over the wave crests as carbonate sands and corbulid granules were draped over the structure during deposition. The upper corbulid laminae are convex upward and dip downstream. The dips of the laminae are after Allen (1982, his figures 10–21) and the elongate particle imbrication matches the work of Yagishita and Taira (1989).

(upper part has been called Gillespie Sand) somewhere in the eastern part of Kerr County but before or roughly at the southern border of Gillespie County. The distance from Big Joshua Creek to where the *Corbula* bed vanishes to the north is a least 25 km. The question is whether there was enough relief to trigger a mass flow in this way. Postma (1984) generally shows slopes of 5–14°. In relation to massive versus stratified deposits, the poorly sorted corbulid granules suspended in a coarse carbonate sand matrix best matches the massive pebbly sandstones found in steeper unstable proximal deltas (Postma, 1984). The suspended clasts within the matrix become more organized and stratified in the distal parts of debris flows. Thus, the paleoslope is problematic. A storm might generate a sudden influx of runoff and a surge of rapid prograding sediments that could trigger a debris flow. Intense wave action and liquefaction have been caused by intense waves (Allen, 1982b). In Spain, soft sediment deformation structures including load casts and water structures have been interpreted to be caused by tempestite deposits associated with large storm waves (Molina et al., 1998). But then again, the close association with antidunes is problematic for a storm trigger. Besides large waves, overloading and slumping processes; earthquakes and tsunamis also cause liquefaction and deformation (Molina et al., 1998).

The cyclic nature of the Glen Rose Formation is due to episodic tectonic activity in the detrital source area (Lozo and Stricklin, 1956). Each time the Llano Uplift rejuvenated itself, terrigenous detrital material entered the sea followed by an extremely shallow, turbulent, carbonate phase (Lozo and Stricklin, 1956). It is likely that some of these rejuvenations were accompanied by earthquakes, which easily disrupts sediments and the acceleration rate due to gravity. Seismic shaking and vibrations cause liquefaction and sand volcanoes (Bolt, 1993; Molina et al., 1998). Pore-water pressure between sand grains turns sandy material into a dense liquid (Bolt, 1993). The debris flow dislodges by hydroplaning down the low-angle slope because earthquake waves reduce gravity to practically nil (Bolt, 1993). In a subaqueous environment water slips beneath the swift-moving debris flow head leading to higher velocities as the debris flow

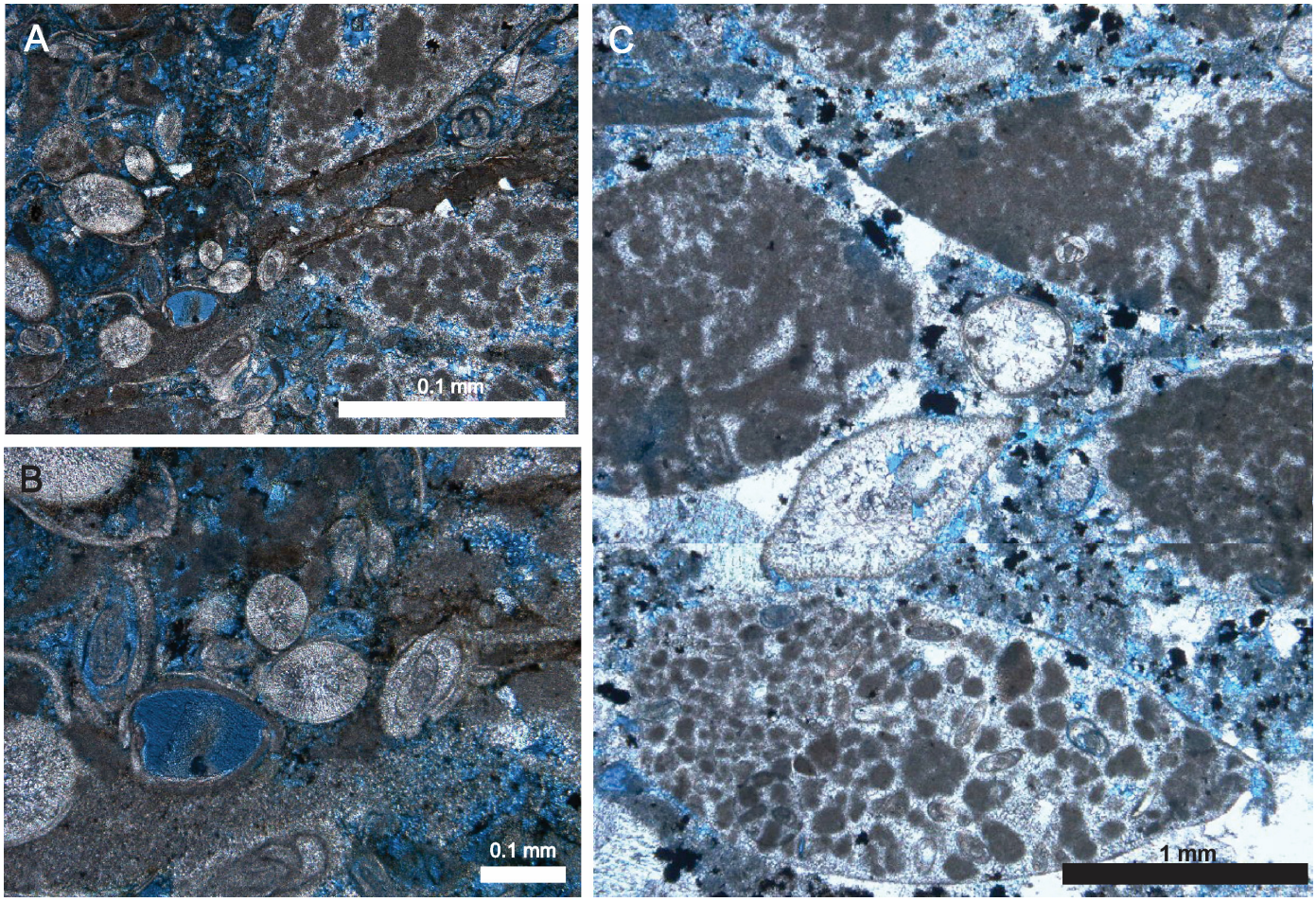

Figure 13. Photomicrographs of particles from a thin section made from the Blanco River sample taken from the antidune imaged in Figures 11B and 12 A. (A) Coarse (approximately 3 mm long) corbulids caught up with finer particles including ostracods, miliolids, peloids, and small pockets of micrite caught between grains suggesting sudden deposition from a high-energy event. (B) Zoomed image of the center left of (A) showing ostracods, some filled with marine cement, and miliolid foraminifera. (C) Corbulid shells in biosparite/packstone. The lower shell is filled with blocky calcite spar cement, peloids, and miliolids. The small middle shell is filled with bladed grading to blocky calcite cement. Peloids fill the upper shells to the left and right. Opaque crystals between corbulid shells were identified as pyrite using reflected light.

hydroplanes across the substrate (Marr et al., 2001). This leads to flow transformations and vertical transverse tension cracks. Marr et al. (2001) demonstrated that when the cracks extend into the underlying bed, blocks become detached from the main flow and slide as separate pieces as seen in Figures 5A and 6A. As the debris flow comes to a halt, the separated pieces and sediments within the flow collide. This is what caused the front side of some blocks to slide on top of the backside of others as depicted in Figures 6A and 6B.

The underlying liquified coarse carbonate sand deforms beneath these blocks in Figures 5A and 6A as sand volcanoes erupted into the overlying dense debris flow (Marr et al., 2001). In a deep ocean environment, giant water-escape structures of the same manner were found in competent sediment gravity flows caused by earthquakes (Johns et al., 1981). They formed by the upward injection of over-pressurized watery sediments caused by loading of the overlying deposit (Johns et al., 1981). The hummocky surfaces, internal deformation, ridges between slide blocks, and even the lenticular structures in Figures 5 and 6 were formed by compression and loading when the flow stopped (Marr et al., 2001). Based on the 40–70° transverse strike of the cracks between the load-flow structures (i.e., debris flow slide blocks) and the collision pattern especially seen in Figure 6A, the debris flow moved from the northwest down a gentle slope towards the southeast. The debris flow in the *Corbula* sequence is a localized effect, which demonstrates that this location was closer to the tectonic source. A submarine earthquake and tsunami does explain both the debris flow and antidunes.

The Tsunami

Tsunamis cause abrupt changes in current direction at right angles and opposed to the seabed slope (Coleman, 1968; Dawson and Stewart, 2008). In the *Corbula* bed, diversion of the current is displayed in the upper antidune bed that overrode the lower antidune beds. The current moved from the southwest towards the northeast. With antidunes, greater wavelengths mean higher current velocities (e.g., Middleton, 1965; Hand, 1974; Allen, 1982a; Barwis and Hayes, 1985). The greatest wavelengths approaching 60 cm occur at Big Joshua Creek, Kendall County, and at Hamilton Creek, Travis County. At the Blanco River site and Canyon Lake Gorge, the current slowed down somewhat because the wavelength reduced to 45 cm or about 20%. At Canyon Lake Gorge, a current flowing north, which is opposite of the regional slope, must have been particularly strong because the northeast current was rotated counterclockwise 45° as Figure 9 displays.

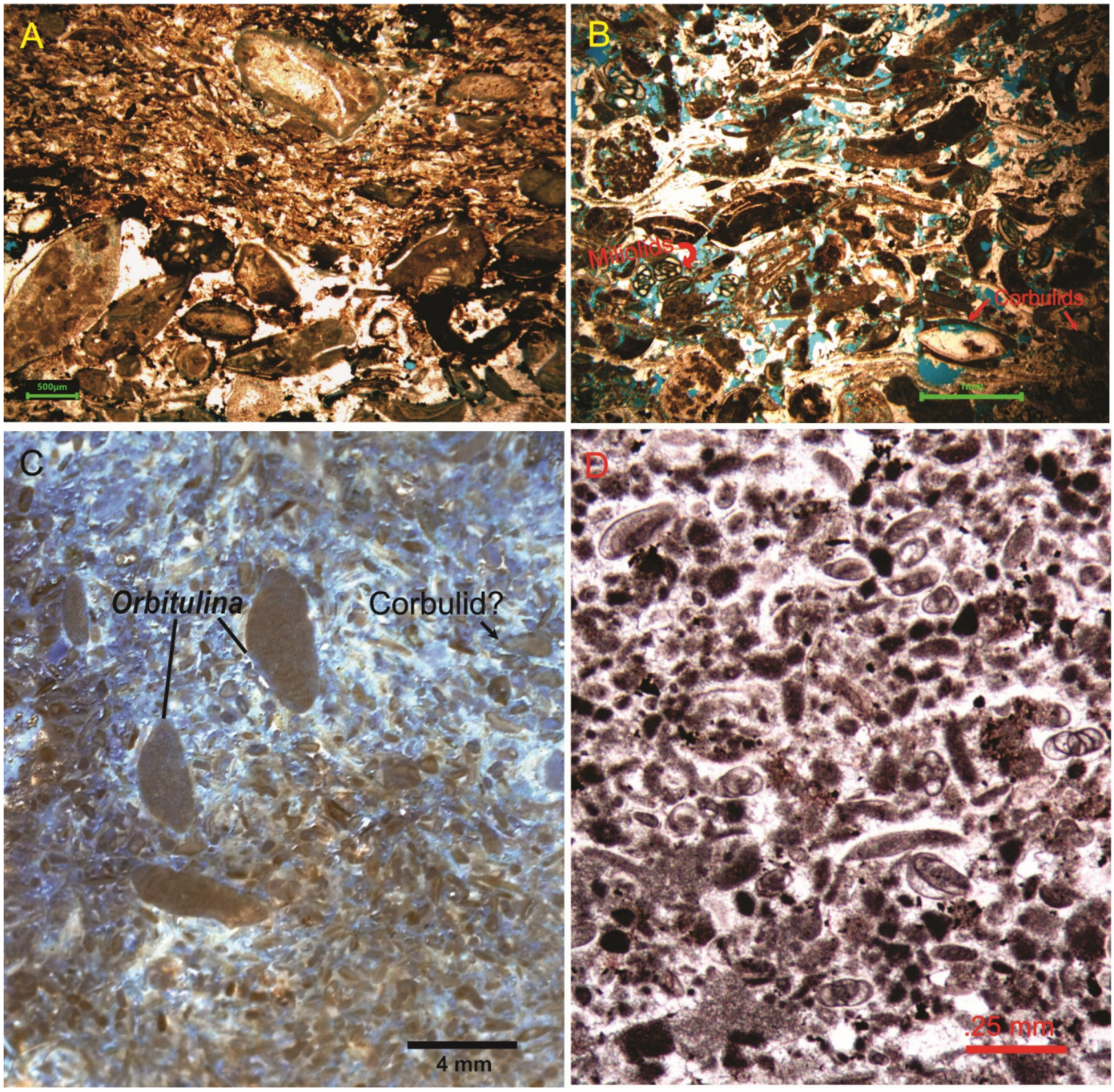

Figure 14. Photomicrographs of particles reflecting high energy in the *Corbula* beds. (A) Canyon Lake Gorge. Coarse imbricated corbulids (above scale bar) and mostly fines in upper part of thin section. Dip of corbulids to the left is upcurrent. Particles within the fines appear to dip to the right in the opposite direction. (B) Little Blanco River. A variety of particles including algal debris, miliolid foraminifera shell fragments, peloids, and corbulids; most elongate particles dipping to the left. (C) Middle Creek Roadcut. This is not a thin section but rather macrophotography of a polished slab including color inversion for a better view of particles. No definitive corbulids could be found, but *Orbitulina texana* are present in a matrix of smaller, rounded grains many with a micritic coating. High energy is indicated by the unnatural edgewise position of the *Orbitulina* fossils. (D) Twin Sisters Roadcut. Miliolids and peloids occur in a 1 cm thick mudstone (to the naked eye the rock looks like shale). Instead, it is a fine-grained packstone with silt-size particles and represents the waning stage between successive tsunami waves.

Perhaps the northward flowing current was high tide that combined its strength with the northeastward flowing current. On the other hand, tsunami waves can attack from more than one direction. The first set of gigantic waves from the 1992 Flores tsunami invaded Babi Island from the northwest; this was followed by a second wave from the southwest, a difference of about 90° (Minoura et al., 1992).

A tsunami explains currents moving towards the west at 280° and towards the south at the same time. Before a tsunami arrives onshore, there is a rapid withdrawal of the sea (Davidson-

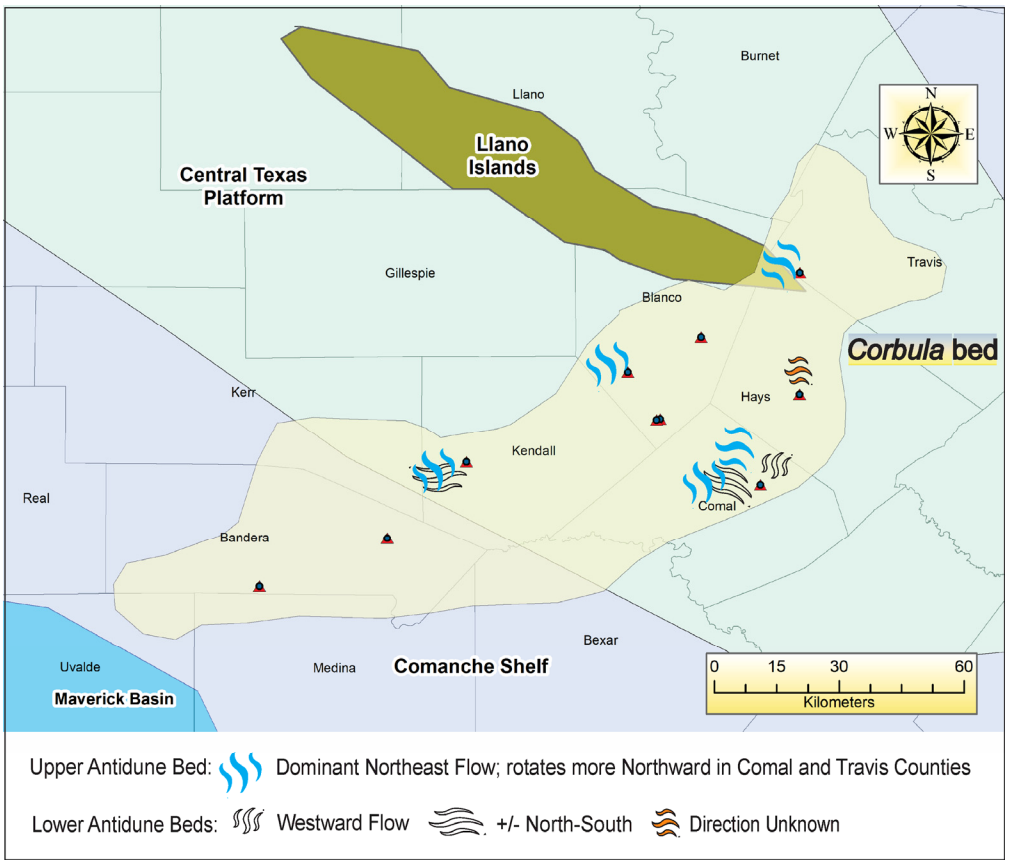

Figure 15. Generalized paleogeographic map with county names. The upper antidune bed (blue waveform) of the *Corbula* bed (tan transparent color) moved northeastward overriding the lower antidune beds. A strong northward current evidenced in the lower bed may have pushed or rotated the current northward at Canyon Lake Gorge, Comal County. The extent of the *Corbula* bed is approximated based on the structure contour datum: *Corbula* bed map of Stricklin et al. (1971, their figure 3, page 8). It is superimposed onto a generalized paleogeographic map compiled from the following maps: early Cretaceous Albian map (Bebout and Loucks, 1974, their page 6 and figure 2, page 7) and the early-middle Albian Comanche Shelf map (Scott et al., 2007, their figure 1, page 182).

Table 3. Generalized tsunami stratigraphy patterns compared.

Chicxulub Tsunami La Lajilla, Northeastern Mexico; onshore (Smit et al., 1994)	*Corbula* Sequence; Lagoon (This Study)	2004 Sumatra-Andaman Tsunami; typical onshore (Phantuwongraj & Choowong, 2012)	Boso Peninsula, East Japan; small bay (Fujiwara & Kamataki, 2008)
Top			
Climbing Ripples	Wavy Beds	Mud Cap	Mud Cap
Massive Fining Upwards	Massive to Crudely Laminar	Upward Thinning and Fining	Fining Upwards
Plane Beds Fining Upwards	Plane Beds Thinning & Fining Upwards (Wavy)	Ripples and Dunes	HCS Mimics* and Lenticular Structures
Antidunes, Linguoid Ripples and Climbing Ripples	Antidunes above Traction Carpet	Antidunes above Traction Carpet	Dunes and Antidunes
Bottom			

***In the same volume, HCS beds are hummock mimics and antidunes (Shiki et al., 2008b).**

Arnott, 2010). This recession or drawback of the shoreline is known to be more than a kilometer (Fritz and Borrero, 2006). Sea level has been observed to drop 5 to 6 m in conjunction with tsunami drawback (Weyl, 1970). If the lagoon still had no more than 6 m of water in it under normal circumstances, then the withdrawal of the sea could have temporarily drained several kilometers of the Central Texas Platform to the west and south. If this is the case, the westward and southward flows in Figures 7 and 8 may represent the sudden recessive movement of water into the tsunami. This explains why the high velocity lunate forms in Figure 7, which also include antidunes (Fig. 11A), represent diminishing water depths. The water feeds the tsunami like a large undertow (Fritz and Borrero, 2006). The first tsunami wave invaded from the south and flowed northward, perhaps around 10° per Figures 7 and 8. The first wave was overridden by the second from the southwest, which flowed northeastward at about 60°. Interference from the colliding currents may have led to eddies and whirlpools. It also reduced the current velocity at Canyon Lake Gorge and at the Blanco River site, but the combined flow, moving roughly 30° further to the northeast caused an increase in velocity at the Hamilton Creek site, Travis County, where the tsunami appears to have overtopped the edge of the Llano islands in Figure 15. The overriding dominant paleocurrent appears to have flowed from the southwest towards the

northeast. This is how antidunes were made over an area of at least 4,000 km^2. Although major storms can drive high velocity currents across shelves, the creation and preservation of antidunes with evidence of diverging current directions over such an extensive area is indicative of a tsunami.

On Figure 15, the linear distance from Big Joshua Creek, Kendall County, through the Blanco River site to Hamilton Creek, Travis County, is about 90 km, and is the approximate path of the northeast flowing paleocurrent. Likewise, the distance from the Blanco River downslope to Canyon Lake Gorge, Comal County, is about 40 km. In shallow waters a tsunami is a powerful swift moving flood of water (Garrison and Ellis, 2016). On the shelf, tsunami deposits can be confused with those from a flooding river mouth (Bourgeois, 2009). This tsunami flood that eroded and deposited the *Corbula* bed was at least 40 km wide and 90 km in distance based on the outcrop evidence. Abundant visual observations of tsunamis in nearshore environments indicate turbidity and current velocities of several meters per second (Coleman, 1968; Sugawara et al., 2008; Bourgeois, 2009).

A quick way to estimate velocity is by taking the square root of the product of gravity (9.8 m/s^2) multiplied by water depth (Garrison and Ellis, 2016). If the mean depth of the lagoon was 4 m, then the velocity equates to about 6 m/s, which is reasonable. Even onshore in Australia, a raging tsunami wall of turbulent water 7.5–12 m high flowed inland across the terrain at speeds of 7–8 m/s (Bryant and Nott, 2001). The movement is uniform through the water column except along the sea floor (Sugawara et al., 2008). The current along the sea floor causes shear and strong tractive forces, which leads to deep erosion, lifting, and turbulence (Sugawara et al., 2008). As this happens eddies and vortices occur above the sharp erosive contact in the boundary layer (Sugawara et al., 2008). Some swept-up particles are then transported as bed load and those lifted in the overlying current is the suspended load (Sugawara et al., 2008). Bed load is transported as rapid interactions with the sea floor, but at lower velocities (boundary layer) than particles that are lifted into the overlying suspended load (Sugawara et al., 2008). If the tsunami did flow across the platform at 6–8 m/s, all that was needed to erode corbulid granules into traction at the seabed was 1.5–2 m/s (Thornton, 1978). Most corbulids were caught up in the eddies and vortices of the boundary layer to form antidunes. Other corbulids were lifted higher into the suspended load. It is evident that both traction and suspension processes formed the *Corbula* sequence.

The stacking pattern of the *Corbula* sequence compares to that of other tsunamis, but there are nomenclature issues regarding the descriptions of beds in a tsunami sand sheet. Most descriptions of sedimentary structures are from the onshore part of a tsunami deposit. Nevertheless, many features are the same. In one case, current ripples, comprised of medium-coarse sand, are deposited directly above a sharp erosional undulating surface (Nanayama, 2008). These current ripples include erosional troughs with symmetrical lamina filling troughs, and other structures with up-current dipping lamina, convex upward structures (hummocks) and downdip lamina that truncates other structures. By comparing these with photographs and figures in Alexander et al. (2001) reveals that the current ripples are three-dimensional antidunes. Nanayama (2008) stated that the particles that ended up in these ripple forms were transported by tractive currents. They mimic the density underflows of turbidity currents on an erodible bed (e.g., Hand, 1974). The general tsunami model and other sites characteristically have antidunes in basal beds of a tsunami deposit (Fujiwara, 2008; Fujiwara and Kamataki, 2008). The swift moving density current produces antidunes (Shiki et al., 2008b). The 2004 Indian Ocean tsunami deposit produced a traction carpet upon which antidunes were deposited (Phantuwongraj and Choowong, 2012). Based on this evidence, it becomes likely that the antidunes in the lower half of the *Corbula* sequence (or *Corbula* type bed) were formed by high density bedload tractive currents with the aid of suspension processes. The problem involves the densities and velocities of the bed load versus the suspended load (e.g., Bourgeois, 2009). In a flume, fluvial antidunes form at greater velocities than plane beds (Middleton, 1965; Allen, 1982a; Cartigny et al., 2014). For example, in Figure 10B the traction carpet may be the beds that underlie the mound shape antidunes, which in its final form was caused by suspension related velocities. Then the overlying wavy beds that thin and fine upwards in Figure 10C were caused by waning currents from the suspended load at lower velocities than the mound shaped antidunes. But for short-crested antidunes, Hand (1974, his page 646) felt that there must be a "density discontinuity" within the turbidity current. In this regard, a tsunami would have a less dense turbidity current riding above a denser turbidity current near the sea floor. The lower half of the *Corbula* sequence represents the denser flow with traction and the upper half is suspended load fallout that buried the antidunes.

Rapid burial of the lower half of the *Corbula* sequence is evidenced in the overlying friable wackestone-packstone, which covered the antidune beds during the waning stages of the event as depicted in Figure 2. Most particles in a tsunami end up in suspension before being deposited (Sugawara et al., 2008), which is also evidenced in antidune flume studies when these particles rise in plumes related to breaking antidunes and hydraulic jumps (e.g., Alexander et al., 2001; Cartigny et al., 2014). Some of the suspended fraction could have come from distal sources. This happens because a tsunami can affect sediments 1000 m deep (Coleman, 1968). Because the flow speed is faster in the turbulent suspension than it is along the sea floor, the suspended fraction can bypass the denser tractive currents below. The tremendous disturbance by tsunami currents in nearshore waters continues to exceed 5 m/s for many hours, including sloshing and seiche in semi-enclosed bodies of water (e.g., Coleman, 1978). Over the course of hours beds became thinner and finer upwards. This is because silt and clay size particles stay in suspension longer than sand size or coarser materials, and thereby represent waning or stagnant conditions between tsunami wave incursions (e.g., Fugiwara and Kamataki, 2008; Lewis and McConchie, 1994; Sugawara et al., 2008). The overlying soft wackestone-packstone is crudely laminated to massive with abundant sand-size particles and marine megafossils. Laminations often form in association with antidunes (Hand, 1974). At Bang Sak beach, Thailand, the 2004 tsunami deposited 33 cm of coarse, poorly sorted sand with vague laminations above the 10 cm thick very coarse deposit with shell and coral debris (Goto et al., 2008). Laminations indicate a dominating flow direction like antidunes while massive beds reflect severe mixing due to high turbulence and rapid deposition (Fujiwara, 2008; Sugawara et al., 2008; Cartigny et al., 2014). A thin hard wavy bed, a few centimeters thick with corbulids or ostracods caps the wackestone. A combination of diverting currents and continuous rapid sedimentation protected the antidune beds of the lower half of the *Corbula* sequence. Scattered imbricated corbulids and small flame structures in a sample from one of these finer grained wavy plane beds at the Blanco River site indicates a flow reversal back to the southwest, an area closer to the origin of the tsunami. This Blanco River sample matches the wackestone sample, with poorly sorted corbulids, gathered at Williams Creek, Bandera County, and confirms that fines were carried towards the southwest (e.g., Stricklin et al., 1971). Tsunami backwash is commonly a poorly sorted sandy mud (Sugawara et al., 2008). Accumulated backwash may be typical of the tsunami deposits in Bandera County. Different types of tsunami deposits caused by the same tsunami depend on a variety of factors including localized changes in the geology and geomorphology (e.g., Smit et al., 1994; Dawson and Stewart, 2008). This is because a tsunami is as much of an erosive event as it is a depositional one (Keating et al., 2008). Antidunes are considered more of an erosional scour feature rather

than depositional (Keating et al., 2008). In Bandera County, the lower antidunes may not exist because only erosion was taking place in that area.

Some researchers think that the beds that thin and fine above tsunami antidunes are HCS beds (Fujiwara, 2008; Fujiwara and Kamataki, 2008). Climbing current ripples deposited above the basal antidune beds in the tsunami deposit associated with the Chicxulub tsunami are noted to have been misinterpreted previously as HCS (Smit et al., 1994). Apparently, three-dimensional antidunes do indeed resemble HCS (Rust and Gibling, 1990). Alexander et al. (2001) also demonstrate that antidunes come in many different forms. Thus, hummocky and swaley bedforms in tsunami deposits are now considered HCS mimics and antidunes (Shiki et al., 2008b). Table 3 was compiled to illustrate a general comparison of the *Corbula* sequence with other tsunami deposits.

The Llano Uplift is part of a much larger tectonic setting at the time the *Corbula* bed was deposited. Figure 15 indicates that the *Corbula* bed extends all the way to the edge of the Maverick Basin, a southeast-northwest rift basin (Alexander, 2015). It was a rapidly subsiding basin situated at the northwest end of the Rio Grande embayment (Muncey and Drimal, 1993). Across the Rio Grande River into Mexico was the Chihuahua Trough, a major tectonic feature, which inverted later as part of the Laramide Orogeny (Haenggi, 2002). This trough was initially set up by the subduction of the immense Farallon Plate (Padilla y Sanchez, 2017). Rhyolitic igneous activity in the Chihuahua trough occurred during deposition of the Cuchillo Formation (a Glen Rose equivalent), and the major fault along the trough's west side remained active through the early Albian (Haenggi, 2002). The debris flow in the basal *Corbula* bed that moved over a low-angle slope, overtopped by widespread antidunes moving towards the northeast indicates a disturbance (e.g., earthquakes; submarine landslides) somewhere to the southwest associated with one or more of these tectonic structures. Ninety percent of modern tsunamis are directly caused by submarine earthquakes (Sugawara et al., 2008). The catastrophic tectonics associated with the Cretaceous are considered to have been far worse (Ager, 1993; Shiki and Tachibana, 2008). Even small earthquakes and volcanic tremblors can induce slumping of coastal landforms and liquefaction of the sea bottom (Sugawara et al., 2008). Thus, a search for evidence of earthquakes and submarine landslides should be found in equivalent strata within these tectonic structures to southwest unless it was triggered by some other southerly source associated with the formation of the Gulf of Mexico.

CONCLUSION

The *Corbula* sequence is a multibed sheet deposit about 1 m thick, indicative of turbulent processes associated with tsunami erosion and deposition. For simplicity, it can be subdivided into two parts, a hard, lower half with high velocity bedforms and an upper soft, friable unit. The type *Corbula* bed corresponds to the hard-iron stained ledge-forming packstone traceable across Central Texas, the lower half of the sequence. The type bed contains supercritical flow three-dimensional antidunes. The sharp undulating erosion surface with deep scour and load structures completely obliterated the life habitat of the corbulids. They were swept up along with other materials in the underlying beds by strong tractive currents. At some places miliolids, *Orbitulina texana*, fossilized algae and peloids are more common than corbulids. The tsunami simply eroded and redeposited whatever material it encountered. The high-density turbid underflow created antidunes by a tractive scour-and-fill process. Tightly packed corbulids tended to be deposited in zones across the top of antidune wave crests. Some corbulids were lifted higher into the tsunami wave train along with winnowed fines and other debris and were transported by turbulent suspension processes above the high density turbulent tractive current. As energy waned the particles rapidly dropped out of suspension and covered the antidunes. This is evidenced by the upward thinning and fining, laminations and overlying massive-crudely laminated wackestones. The antidunes were preserved by rapid continuous deposition.

It is probable that the trigger for the tsunami was a submarine earthquake to the southwest. Vibrations and shaking would liquify the coarse carbonate sand at Big Joshua Creek. This caused the debris flow to hydroplane towards the southeast down the low-angle regional slope of less than 0.05°. As it slid, cracks formed in the dense flow, some pieces segregated and then collided as the head of the flow came to a stop. The process led to load features of internal deformations, load casts and sand volcanoes. Immediately above the debris flow is the surficial antidune bed with a paleocurrent that flowed to the northeast at about 60°. This same surficial overriding flow direction towards the northeast at the Blanco River site and Canyon Lake Gorge indicates that the flow was at least 40 km wide. The greater wavelength between antidune wave crests at Big Joshua Creek is additional evidence for a trigger source to the southwest because greater wavelength indicates higher velocities. The lower antidune beds are interpreted as tsunami drawdown in which the sea withdrew towards the west, then towards the south. Then, as the overriding northeasterly flow surged across the Central Texas Platform, it encountered another strong current moving north. This effect is likely the first invading tsunami wave. Tsunami drawdown moved south down the regional slope, then back towards the north and may have combined its strength with high tide. The collision of currents could have caused an eddy to form at the Canyon Lake Gorge. The combined flow continued northeast.

The wide size range of corbulids locked together in these antidunes over the large area indicates that they were thriving and reproducing prior to transport and mass burial. The lack of bioturbation in the antidunes or above in the muddier wackestone-packstone layers suggest that they could not escape out of the situation. Apparently, they suffocated in place. Miliolids, peloids, and other particles filled the interiors of their shells, which dissolved later as they became steinkerns.

After the tsunami event, shallow conditions arose. At Canyon Lake Gorge, peritidal conditions wider than typical intertidal conditions are shown for at least the first 6 m of strata deposited above the *Corbula* bed (Ward and Ward, 2007). Ward and Ward (2007) showed stromatolites at two levels above the *Corbula* bed. The first layer sits directly above the *Corbula* bed and a more significant bed occurs at 2 m above it. They also show collapse breccias at about 4 to 5 m above the *Corbula* bed. Perkins (1974) related that the collapse breccias involve gypsum. Therefore, the shallow waters probably became hypersaline after the tsunami event. The combination of large-scale tectonics, subsidence, and the addition of extra sediments brought into the lagoon all played a role in the waters becoming shallower and hypersaline for a time.

The *Corbula* bed has been utilized as a marker bed and cross-section datum for a long time (e.g., Lozo and Stricklin, 1956; Stricklin et al., 1971; Perkins, 1974; Scott, 2007). The evidence presented suggests strongly that the *Corbula* bed is a tsunami deposit. Perhaps, it is time to revisit other marker beds in the geologic record in the light of tsunami research.

ACKNOWLEDGMENTS

The lead author would like to thank his wife, Selene Sigler, and Tim Crosson for their assistance at outcrops especially with field equipment and photography. We are grateful to the Gorge Preservation Society, Canyon Lake, Texas, especially Jaynellen Kerr, for granting us access to and providing field guides Jim Dyess and Pete Bryant to assist at the Canyon Lake Gorge. During the review process, the critiques of Alton Brown and Art Saller, proved to be invaluable to the research and writing of this

paper. They have our utmost gratitude. Besides this, Selene deserves a lot of praise for her patience during the research and writing of this paper.

REFERENCES CITED

Ager, D. V., 1993, The nature of the stratigraphic record, 3rd ed.: John Wiley & Sons, West Sussex, England, 151 p.

Allen, J. R. L., 1982a, Sedimentary structures, their character and basis, v. I: Elsevier, Amsterdam, The Netherlands, 593 p.

Allen, J. R. L., 1982b, Sedimentary structures, their character and basis, v. II: Elsevier, Amsterdam, The Netherlands, 663 p.

Alexander, J., J. S. Bridge, R. J. Cheel, and S. F. LeClair, 2001, Bedforms and associated sedimentary structures formed under supercritical water flows over aggrading sand beds: Sedimentology, v. 48, p. 133–152.

Alexander, M., 2015, A new look at Maverick Basin basement tectonics: Bulletin of the South Texas Geological Society, v. 55, no. 6, p. 32–45.

Asquith, G. B., 1979, Subsurface carbonate depositional models: A concise review: PennWell Publishing Company, Tulsa, Oklahoma, 121 p.

Barker, R. A., P. W. Bush, and E. T. Baker, 1994, Geologic history and hydrogeologic setting of the Edwards-Trinity aquifer system, west-central Texas: U.S. Geological Survey Water-Resources Investigations Report 94–4039, Austin, Texas, 51 p.

Barnes, V. E., 1967, Geology of the Yeager Creek quadrangle, Blanco County: Bureau of Economic Geology, Austin, Texas, scale 1:24,000.

Barnes, V. E., project director, 1974, Geologic atlas of Texas: Austin sheet, Francis Luther Whitney memorial ed.: Bureau of Economic Geology, Austin, Texas, reprinted 1995, scale 1:250,000.

Barnes, V. E., project director, 1981, Geologic atlas of Texas: Llano Sheet, Virgil E. Barnes ed., 1:250,000 scale: Bureau of Economic Geology, Austin, Texas, reprinted 1986.

Barnes, V. E., project director, revised 1982, Geologic atlas of Texas: San Antonio sheet, Robert Hamilton Cuyler memorial ed.: Bureau of Economic Geology, Austin, Texas, scale 1:250,000.

Barwis, J. H., and M. O. Hayes, 1985, Antidunes on modern and ancient washover fans: Journal of Sedimentary Petrology, v. 55, p. 907–916.

Bebout, D. G., and R. G. Loucks, 1974, Stuart City Trend, Lower Cretaceous, South Texas: A carbonate shelf-margin model for hydrocarbon exploration: Bureau of Economic Geology Report of Investigations 78, Austin, Texas, 84 p.

Bebout, D. G., and R. G. Loucks, 1983, Lower Cretaceous reefs, South Texas, *in* P. A. Scholle, D. G. Bebout, and C. H. Moore, eds., Carbonate depositional environments: American Association of Petroleum Geologists Memoir 33, Tulsa, Oklahoma, p. 441–444.

Bolt, B. A., 1993, Earthquakes, newly revised and expanded: W. H. Freeman and Company, New York, 331 p.

Bourgeois, J., 2009, Chapter 3. Geologic effects and records of tsunamis, *in* A. R. Robinson and E. N. Bernard, eds., The sea, v. 15: Tsunamis: Harvard University Press, Cambridge, Massachusetts, p. 53–91.

Brenchley, P. J., and G. Newall, 1970, Flume experiments on the orientation and transport of models and shell valves: Palaeogeography, Palaeoclimatology, Palaeoecology, v. 7, p. 185–220.

Bryant, E. A., and J. Nott, 2001, Geological indicators of large tsunami in Australia: Natural Hazards, v. 24, p. 231–249.

Cartigny, M. J. B., D. Ventra, G. Postma, and J. H. Van Den Berg, 2014, Morphodynamics and sedimentary structures of bedforms under supercritical flow conditions: New insights from flume experiments: Sedimentology, v. 61, p. 712–748.

Chakrabarti, A., 2005, Sedimentary structures of tidal flats: A journey from coast to inner estuarine region of eastern India: Journal of Earth System Science, v. 114, p. 353–368.

Coleman, P. J., 1968, Tsunamis as geological agents: Journal of the Geological Society of Australia, v. 15, p. 267–273.

Coleman, P. J., 1978, Tsunami sedimentation, *in* R. W. Fairbridge and J. Bourgeois, eds., The encyclopedia of sedimentology: Dowden, Hutchinson and Ross, Stroudsburg, Pennsylvania, p. 828–831.

Davidson-Arnott, R., 2010, Introduction to coastal processes and geomorphology: Cambridge University Press, U.K., 442 p.

Dawson, A. G., and I. Stewart, 2008, Offshore tractive current deposition: The forgotten tsunami sedimentation process, *in* T. Shiki, Y. Tsuji, T. Yamazaki and K. Minoura, eds., Tsunamiites: Features and implications: Elsevier, Amsterdam, The Netherlands, p. 153–161.

Dott, R. H., and J. Bourgeois, 1982, Hummocky stratification: Significance of its variable bedding sequences: Geological Society of America Bulletin, v. 93, p. 663–680.

Folk, R. L., 1980, Petrology of sedimentary rocks: Hemphill Publishing Company, Austin, Texas, 182 p.

Fritz, H. M., and J. C. Borrero, 2006, Somalia field survey after the December 2004 Indian Ocean tsunami: Earthquake Spectra, v. 22, p. 219–233.

Fujino, S., H. Naruse, A. Suphawajruksakul, T. Jarupongsakul, M. Murayama, and T. Ichihara, 2008, Thickness and grain-size distribution of Indian Ocean tsunami deposits at Khao Lak and Phra Thong Island, south-western Thailand, *in* T. Shiki, Y. Tsuji, T. Yamazaki and K. Minoura, eds., Tsunamiites: Features and implications: Elsevier, Amsterdam, The Netherlands, p. 123–132.

Fujiwara, O., 2008, Bedforms and sedimentary structures characterizing tsunami deposits, *in* T. Shiki, Y. Tsuji, T. Yamazaki and K. Minoura, eds., Tsunamiites: Features and implications: Elsevier, Amsterdam, The Netherlands, p. 51–62.

Fujiwara, O., and T. Kamataki, 2008, Tsunami depositional processes reflecting the waveform in a small bay: Interpretation from the grain-size distribution and sedimentary structures, *in* T. Shiki, Y. Tsuji, T. Yamazaki and K. Minoura, eds., Tsunamiites: Features and implications: Elsevier, Amsterdam, The Netherlands, p. 133–152.

Försich, F. T., and Y. Pan, 2016, Diagenesis of bivalves from Jurassic and Lower Cretaceous lacustrine deposits of northeastern China: Geological Magazine, v. 153, p. 17–37.

Garrison, T., and R. Ellis, 2013, Oceanography: An invitation to marine science, 9th ed.: Cengage Learning, Boston, Massachusetts, 604 p.

Goto, K., F. Imamura, N. Keerthi, P. Kunthasap, T. Matsui, K. Minoura, A. Ruangrassamee, D. Sugawara, and S. Supharatid, 2008, Distribution and significance of the 2004 Indian Ocean tsunami deposits: Initial results from Thailand and Sri Lanka, *in* T. Shiki, Y. Tsuji, T. Yamazaki and K. Minoura, eds., Tsunamiites: Features and implications: Elsevier, Amsterdam, The Netherlands, p. 105–122.

Haenggi, W. T., 2002, Tectonic history of the Chihuahua Trough, Mexico and adjacent USA, part II: Mesozoic and Cenozoic: Bulletin of the Geological Society of Mexico, v. 55, no. 1, p. 38–94.

Hand, B., 1974, Supercritical flow in density currents: Journal of Sedimentary Petrology, v. 44, p. 637–648.

Häntzschel, W., and R. W. Frey, 1978, Bioturbation, *in* R. W. Fairbridge and J. Bourgeois, eds., The encyclopedia of sedimentology: Dowden, Hutchinson and Ross, Stroudsburg, Pennsylvania, p. 68–71.

Holland, C. H., 1960, Load-cast terminology and origin of convolute bedding: Some comments: Geological Society of America Bulletin, v. 71, p. 633–634.

Johns, D. R., E. Mutti, J. Rosell, and M. Séguret, 1981, Origin of thick, redeposited carbonate bed in Eocene turbidites of the Hecho Group, south-central Pyrenees, Spain: Geology, v. 9, p. 161–164.

Keating, B. H., M. Wanink, and C. E. Helsley, 2008, Introduction to a tsunami-deposits database, *in* T. Shiki, Y. Tsuji, T. Yamazaki and K. Minoura, eds., Tsunamiites: Features and implications: Elsevier, Amsterdam, The Netherlands, p. 359–381.

Leeder, M. R., 1982, Sedimentology: Process and product: George Allen & Unwin, London, U.K., 344 p.

Lewis, D. W., and D. McConchie, 1994, Practical sedimentology, 2nd ed.: Chapman & Hall, New York, 213 p.

Lewy, Z., and C. Samtleben, 1979, Functional morphology and palaeontological significance of the conchiolin layers in corbulid pelecypods: *Lethaia*, v. 12, p. 341–351.

Lozo, F. E., and F. L. Stricklin, Jr., 1956, Stratigraphic notes on the outcrop basal Cretaceous, Central Texas: Gulf Coast Association of Geological Societies Transactions, v. 6, p. 67–78.

Marr, J. G., P. A. Huff, G. Shanmugam, and G. Parker, 2001, Experiments on subaqueous sandy gravity flows: The role of clay and water content in flow dynamics and depositional structures: Geological Society of America Bulletin, v. 113, p. 1377–1386.

Middleton, G. V., 1965, Antidune cross-bedding in a large flume: Journal of Sedimentary Petrology, v. 35, p. 922–927.

Middleton, G. V., 1978, Flow regimes, *in* R. W. Fairbridge and J. Bourgeois, eds., The encyclopedia of sedimentology: Dowden, Hutchinson and Ross, Stroudsburg, Pennsylvania, p. 330–333.

Minoura, K., F. Imamura, T. Takahashi and N. Shuto, 1997, Sequence of sedimentation processes caused by the 1992 Flores tsunami: Evidence from Babi Island: Geology, v. 25, p. 523–526.

Molina, J. M., P. Alfaro, M. Moretti and J. M. Soria, 1998, Soft-sediment deformation structures induced by cyclic stress of storm waves in tempestites (Miocene, Guadalquivir Basin, Spain): *Terra Nova*, v. 10, p. 145–150.

Muncey, G., and C. E. Drimal, 1993, Evaluation of target reservoirs for horizontal drilling: Lower Glen Rose Formation, South Texas: Proceedings of Fuels Technology Contractors Review Meeting, DOE/MC/28239–94/C0327: National Technical Information Service, Springfield, Virginia.

Nagle, J. S., 1968, Glen Rose cycles and facies, Paluxy River valley, Somerville County, Texas: Bureau of Economic Geology Geological Circular 68–1, Austin, Texas, 25 p.

Nanayama, F., 2008, Sedimentary characteristics and depositional processes of onshore tsunami deposits, *in* T. Shiki, Y. Tsuji, T. Yamazaki, and K. Minoura, eds., Tsunamiites: Features and implications: Elsevier, Amsterdam, The Netherlands, p. 63–80.

Nelson, C. H., 1981, Modern shallow-water graded sand layers from storm surges, Bering Shelf: A mimic of Bouma sequences and turbidity systems: Journal of Sedimentary Petrology, v. 52, p. 537–545.

Padilla y Sánchez, R. J., 2017, The Late Triassic–Late Cretaceous flooding of the Gulf of Mexico from the Pacific through Mexico: American Association of Petroleum Geologists Search and Discovery Article 30504, Tulsa, Oklahoma, 7 p., <http://www.searchanddiscovery.com/pdfz/documents/2017/30504padilla/ndx_padilla.pdf.html>.

Phantuwongraj, S., and M. Choowong, 2012, Tsunamis versus storm deposits from Thailand: Natural Hazards, v. 63, p. 31–50.

Perkins, B. F., 1974, Paleoecology of a rudist reef complex in the Comanche Cretaceous Glen Rose Limestone of Central Texas: Geoscience and Man, v. 8, p. 131–173.

Peters, R., and B. Jaffe, 2010, Identification of tsunami deposits in the geologic record: Developing criteria using recent tsunami deposits: United States Geological Survey Open-File Report 2010–1239, Reston, Virginia, 39 p, <https://pubs.usgs.gov/of/2010/1239/of2010-1239.pdf>.

Pitman, J. G., 1989, Stratigraphy of the Glen Rose Formation, western Gulf Coastal Plain: American Association of Petroleum Geologists Search and Discovery Article 91029, Tulsa, Oklahoma, 1 p., <http://www.searchanddiscovery.com/abstracts/html/1989/gcags/abstracts/1190.htm>.

Plummer, F. B., 1950, The Carboniferous rocks of the Llano region of Central Texas: University of Texas Publication 4329, Bureau of Economic Geology, Austin, Texas, p. 101–113.

Putra, P. S., Y. Nishimura, and E. Yulianto, 2013, Sedimentary features of tsunami deposits in carbonate-dominated beach environments: A case study from the 25 October 2010 Mentawai tsunami: Pure and Applied Geophysics, v. 170, no. 9–10, p. 1583–1600.

Rees, A. I., 1968, The production of preferred orientation in a concentrated dispersion of elongated and flattened grains: Journal of Geology, v. 76, p. 457–465, <http://doi.org/10.1086/627343>.

Ricci Lucchi, F., 1995, Sedimentographica: Photographic atlas of sedimentary structures, 2nd ed.: Columbia University Press, New York, 255 p.

Rust, B. R., and M. R. Gibling, 1990, Three-dimensional antidunes as HCS mimics in a fluvial sandstone: The Pennsylvanian South Bar Formation near Sydney, Nova Scotia: Journal of Sedimentary Petrology, v. 60, p. 540–548.

Scott, R. W., 2007, Key bivalves of the Lower Albian Glen Rose Formation, Texas, U.S.A., *in* R. W. Scott, ed., Cretaceous rudists and carbonate platforms: Environmental feedback: Society of Economic Paleontologists and Mineralogists (Society for Sedimentary Geology) Special Publication 87, Tulsa, Oklahoma, p. 247–252.

Scott, R. W., A. M. Molineux, H. Löser, and E. A. Mancini, 2007, Lower Albian sequence stratigraphy and coral buildups: Glen Rose Formation, Texas, U.S.A., *in* R. W. Scott, ed., Cretaceous rudists and carbonate platforms: Environmental feedback: Society of Economic Paleontologists and Mineralogists (Society for Sedimentary Geology) Special Publication 87, Tulsa, Oklahoma, p. 181–191.

Scott, R. W., Z. Wang, X. Lai, and Y. Wang, 2016, Late Albian cactus in shallow carbonate shelf, West Texas: *Carnets de Géologie*, Madrid, v. 16, p. 337–347.

Selley, R. C., 1988, Applied sedimentology: Academic Press Limited: London, U.K., 446 p.

Shanmugam, G., 2006, The tsunamiite problem: Journal of Sedimentary Research, v. 76, p. 718–730.

Shiki, T., K. Minoura, Y. Tsuji, and T. Yamazaki, 2008, Introduction: Why a book on tsunamiites, *in* T. Shiki, Y. Tsuji, T. Yamazaki and K. Minoura, eds., Tsunamiites: Features and implications: Elsevier, Amsterdam, The Netherlands, p. 1–4.

Shiki, T., T. Tachibana, O. Fujiwara, K. Goto, F. Nanayama, and T. Yamazaki, 2008b, Characteristic features of tsunamiites, *in* T. Shiki, Y. Tsuji, T. Yamazaki and K. Minoura, eds., Tsunamiites: Features and implications: Elsevier, Amsterdam, The Netherlands, p. 319–340.

Shiki, T., and T. Tachibana, 2008, Sedimentology of tsunamiites reflecting chaotic events in the geologic record—Significance and problems, *in* T. Shiki, Y. Tsuji, T. Yamazaki and K. Minoura, eds., Tsunamiites: Features and implications: Elsevier, Amsterdam, The Netherlands, p. 341–357.

Shiki, T., and T. Yamazaki, 2008, The term 'tsunamiite,' *in* T. Shiki, Y. Tsuji, T. Yamazaki and K. Minoura, eds., Tsunamiites: Features and implications: Elsevier, Amsterdam, The Netherlands, p. 5–7.

Skipper, K., 1971, Antidune cross-stratification in a turbidite sequence, Cloridorme Formation, Gaspé, Quebec: Sedimentology, v. 17, p. 51–68.

Smit, J., A. Montanari, and W. Alvarez, 1994, Tsunami-generated beds at the KT boundary in northeastern Mexico, *in* G. Keller, W. Stinnesbeck, T. Adatte, N. MacLeod, and D. Lowe, eds., Field guide to the Cretaceous-Tertiary boundary sections in northeastern Mexico: Lunar and Planetary Institute Contribution 827, University of Houston, Clear Lake, Texas, p. 95–101.

Stricklin, Jr., F. L., C. I. Smith, and F. E. Lozo, 1971, Stratigraphy of Lower Cretaceous Trinity deposits of Central Texas: Bureau of Economic Geology Report of Investigations 71, Austin, Texas, 63 p.

Sugawara, D., K. Minoura, and F. Imamura, 2008, Tsunamis and tsunami sedimentation, *in* T. Shiki, Y. Tsuji, T. Yamazaki and K. Minoura, eds., Tsunamiites: Features and implications: Elsevier, Amsterdam, The Netherlands, p. 9–49.

Sullwold, H. H., Jr., 1959, Nomenclature of load deformation in turbidites: Geological Society of America Bulletin, v. 70, p. 1247–1248.

Sullwold, H. H., Jr., 1960, Load-cast terminology and origin of convolute bedding: Further comments: Geological Society of America Bulletin, v. 71, p. 635–636.

Thornton, C. P., 1978, Paragenesis of sedimentary rocks, *in* R. W. Fairbridge and J. Bourgeois, eds., The encyclopedia of sedimen-

tology: Dowden, Hutchinson and Ross, Stroudsburg, Pennsylvania, p. 533–537.

Twenhofel, W. H., 1932, Treatise on sedimentation, 2nd ed.: Dover Publications, New York, in two volumes, Dover ed., 1961, 926 p.

Ward, W. C., and W. B. Ward, 2007, Stratigraphy of the middle part of the Glen Rose Formation (Lower Albian), Canyon Lake Gorge, Central Texas, U.S.A, *in* R. W. Scott, ed., Cretaceous rudists and carbonate platforms: Environmental feedback: Society of Economic Paleontologists and Mineralogists (Society for Sedimentary Geology) Special Publication 87, Tulsa, Oklahoma, p. 193–210,.

Weyl, P. K., 1970, Oceanography, an introduction to the marine environment: John Wiley & Sons, New York, p. 242–243.

Whitney, M. I., 1952, Some zone marker fossils of the Glen Rose Formation of Central Texas: Journal of Paleontology, v. 26, p. 65–73.

Yagishita, K., and A. Taira, 1989, Grain fabric of a laboratory antidune: Sedimentology, v. 36, p. 1001–1005, <http://doi.org/10.1111/j.1365-3091.1989.tb01537.x>.